# NONLINEAR SPECTROSCOPY

1. Introduction

Spectroscopy comes from the Latin "spectron" for *spirit* or *ghost* and the Greek "σκοπιεν" for *to see*. These roots are very telling, because in molecular spectroscopy you use light to interrogate matter, but you actually never see the molecules, only their influence on the light. Different spectroscopies give you different perspectives. This indirect contact with the microscopic targets means that the interpretation of spectroscopy in some manner requires a model, whether it is stated or not. Modeling and laboratory practice of spectroscopy are dependent on one another, and therefore a spectroscopy is only as useful as its ability to distinguish different models. The observables that we have to extract microscopic information in traditional spectroscopy are resonance frequencies, spectral amplitudes, and lineshapes. We can imagine studying these spectral features as a function of control variables for the light field (amplitude, frequency, polarization, phase, etc.) or for the sample (for instance a systematic variation of the physical properties of the sample).

In complex systems, those in which there are many interacting degrees of freedom and in which spectra become congested or featureless, the interpretation of traditional spectra is plagued by a number of ambiguities. This is particularly the case for spectroscopy of disordered condensed phases, where spectroscopy is the primary tool for describing molecular structure, interactions and relaxation, kinetics and dynamics, and tremendous challenges exist on understanding the variation and dynamics of molecular structures. This is the reason for using nonlinear spectroscopy, in which multiple light-matter interactions can be used to correlate different spectral features and dissect complex spectra. We can resonantly drive one spectroscopic feature and see how another is influenced, or we can introduce time delays to see how properties change with time.

Absorption or emission spectroscopies are referred to as linear spectroscopy, because they involve a weak light-matter interaction with one primary incident radiation field, and are typically presented through a single frequency axis. The ambiguities that arise when interpreting linear spectroscopy can be illustrated through two examples:

1) <u>Absorption spectrum with two peaks.</u>
    Do these resonance arise from different, non-interacting molecules, or are these coupled quantum states of the same molecule? (One cannot resolve couplings or spectral correlations directly).
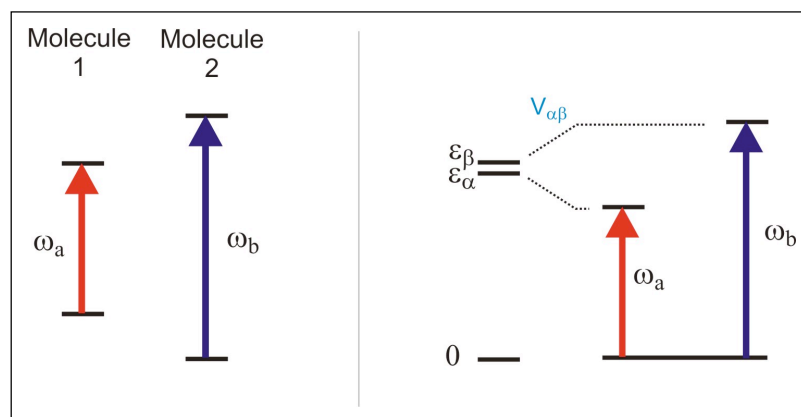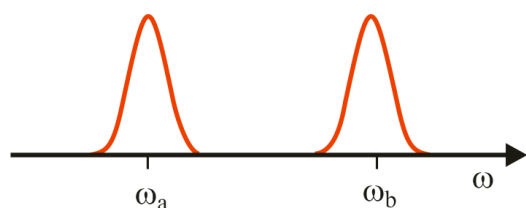
2) <u>Broad lineshapes</u>. Can you distinguish whether it is a homogeneous lineshape broadened by fast irreversible relaxation or an inhomogeneous lineshape arising from a static distribution of different frequencies? (Linear spectra cannot uniquely interpret line-broadening mechanism, or decompose heterogeneous behavior in the sample).
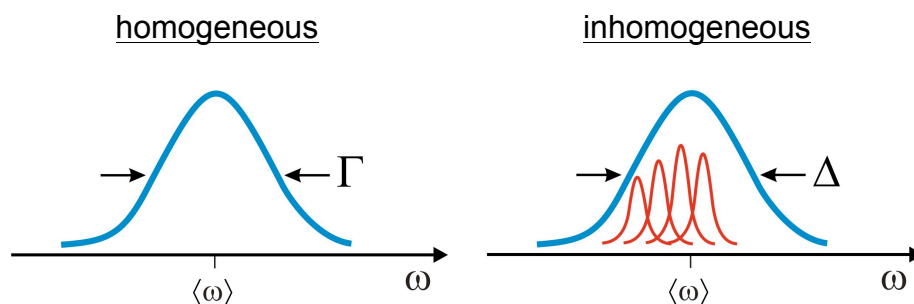
In the end effect linear spectroscopy does not offer systematic ways of attacking these types of problems. It also has little ability to interpret dynamics and relaxation. These issues take on more urgency in the condensed phase, when lineshapes become broad and spectra are congested.
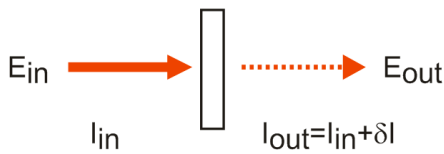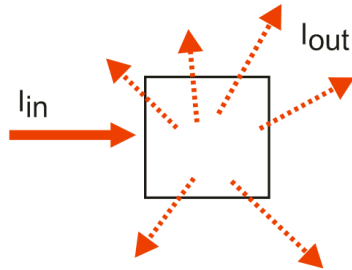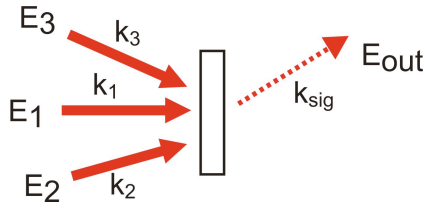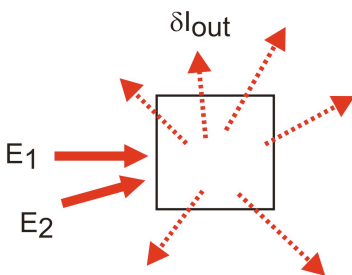
Nonlinear spectroscopy provides a way of resolving these scenarios because it uses multiple light fields with independent control over frequency or time-ordering in order to probe correlations between different spectral features. For instance, the above examples could be interpreted with the use of a double-resonance experiment that reveals how excitation at one frequency ω_1 influences absorption at another frequency ω_2.

What is nonlinear spectroscopy?

Linear spectroscopy commonly refers to light-matter interaction with one primary incident radiation field which is weak, and can be treated as a linear response between the incident light and the matter. From a quantum mechanical view of the light field, it is often conceived as a "one photon in/one photon out" measurement. Nonlinear spectroscopy is used to refer to cases that fall outside this view, including: (1) Watching the response of matter subjected to interactions with two or more independent incident fields, and (2) the case where linear response theory is inadequate for treating how the material behaves, as in the case of very intense incident radiation. If we work within the electric dipole Hamiltonian, nonlinear experiments can be expressed in terms of three or more transition matrix elements. The response of the matter in linear experiments will scale as $|\mu_{ab}|^2$ or $\mu_{ab}\mu_{ba}$, whereas in nonlinear experiments will take a form such as $\mu_{ab}\mu_{bc}\mu_{ca}$. Our approach to describing nonlinear spectroscopy will use the electric dipole Hamiltonian and a perturbation theory expansion of the dipole operator.

2. Coherent Spectroscopy and the Nonlinear Polarization

We will specifically be dealing with the description of coherent nonlinear spectroscopy, which is the term used to describe the case where one or more input fields coherently act on the dipoles of the sample to generate a macroscopic oscillating polarization. This polarization acts as a source to radiate a signal that we detect in a well-defined direction. This class includes experiments such as pump-probes, transient gratings, photon echoes, and coherent Raman methods. However understanding these experiments allows one to rather quickly generalize to other techniques.

Detection:	Coherent	Spontaneous
	$I_{coherent} \propto \left| \sum_i \mu_i \right|^2$ Dipoles are driven coherently, and radiate with constructive interference in direction $\bar{k}_{sig}$	$I_{spont.} \propto \sum_i \left| \mu_i \right|^2$ Dipoles radiate independently $\bar{E}_{sig} \propto \sin\theta$
Linear:	Absorption 	Fluorescence, phosphorescence, Raman, and light scattering
Nonlinear:	 Pump-probe transient absorption, photon echoes, transient gratings, CARS, impulsive Raman scattering	 Fluorescence-detected nonlinear spectroscopy, i.e. stimulated emission pumping, time-dependent Stokes shift

Spontaneous and coherent signals are both emitted from all samples, however, the relative amplitude of the two depend on the time-scale of dephasing within the sample. For electronic transitions in which dephasing is typically much faster than the radiative lifetime, spontaneous emission is the dominant emission process. For the case of vibrational transitions where non-radiative relaxation is typically a picoseconds process and radiative relaxation is a μs or longer process, spontaneous emission is not observed.

The description of coherent nonlinear spectroscopies is rooted in the calculation of the polarization, $\bar{P}$. The polarization is a macroscopic collective dipole moment per unit volume, and for a molecular system is expressed as a sum over the displacement of all charges for all molecules being interrogated by the light

Sum over molecules: $$\bar{P}(\bar{r}) = \sum_m \bar{\mu}_m \delta(\bar{r} - \bar{R}_m) \tag{1}$$

Sum over charges on molecules: $$\bar{\mu}_m \equiv \sum_\alpha q_{m\alpha}(\bar{r}_{m\alpha} - \bar{R}_m) \tag{2}$$

In coherent spectroscopies, the input fields $\bar{E}$ act to create a macroscopic, coherently oscillating charge distribution

$$\bar{P}(\omega) = \chi \bar{E}(\omega) \tag{3}$$

as dictated by the susceptibility of the sample. The polarization acts as a source to radiate a new electromagnetic field, which we term the signal $\bar{E}_{sig}$. (Remember that an accelerated charge radiates an electric field.) In the electric dipole approximation, the polarization is one term in the current and charge densities that you put into Maxwell's equations.

From our earlier description of freely propagating electromagnetic waves, the wave equation for a transverse, plane wave was

$$\bar{\nabla}^2 \bar{E}(\bar{r},t) - \frac{1}{c^2}\frac{\partial^2 \bar{E}(\bar{r},t)}{\partial t^2} = 0 , \tag{4}$$

which gave a solution for a sinusoidal oscillating field with frequency ω propagating in the direction of the wavevector k. In the present case, the polarization acts as a source −an accelerated charge− and we can write

$$\bar{\nabla}^2 \bar{E}(\bar{r},t) - \frac{1}{c^2}\frac{\partial^2 \bar{E}(\bar{r},t)}{\partial t^2} = \frac{4\pi}{c^2}\frac{\partial^2 \bar{P}(\bar{r},t)}{\partial t^2} \tag{5}$$

The polarization can be described by solutions of the form

$$\bar{P}(\bar{r},t) = P(t)\exp\left(i\bar{k}'_{sig}\cdot\bar{r} - i\omega_{sig}t\right) + c.c. \tag{6}$$

As we will discuss further later, the wavevector and frequency of the polarization depend on the frequency and wave vector of incident fields.

$$\bar{k}_{sig} = \sum_n \pm\bar{k}_n \tag{7}$$

$$\omega_{sig} = \sum_n \pm\omega_n \ . \tag{8}$$

These relationships enforce momentum and energy conservation for the problem. The oscillating polarization radiates a coherent signal field, $\bar{E}_{sig}$, in a wave vector matched direction $\bar{k}_{sig}$. Although a single dipole radiates as a *sin θ* field distribution relative to the displacement of the charge,[1] for an ensemble of dipoles that have been coherently driven by external fields, *P* is given by (6) and the radiation of the ensemble only constructively adds along $\bar{k}_{sig}$. For the radiated field we obtain

$$\bar{E}_{sig}(\bar{r},t) = E_{sig}(\bar{r},t)\exp\left(i\bar{k}_{sig}\cdot\bar{r} - i\omega_{sig}t\right) + c.c. \tag{9}$$

This solution comes from solving (5) for a thin sample of length *l*, for which the radiated signal amplitude grows and becomes directional as it propagates through the sample. The emitted signal

$$\bar{E}_{sig}(t) = i\frac{2\pi\omega_s}{nc}l\bar{P}(t)\text{sinc}\left(\frac{\Delta kl}{2}\right)e^{i\Delta kl/2} \tag{10}$$

Here we note the oscillating polarization is proportional to the signal field, although there is a $\pi/2$ phase shift between the two, $\bar{E}_{sig} \propto i\bar{P}$, because in the sample the polarization is related to the gradient of the field. *Δk* is the wave-vector mismatch between the wavevector of the polarization $\bar{k}'_{sig}$ and the radiated field $\bar{k}_{sig}$, which we will discuss more later.

For the purpose of our work, we obtain the polarization from the expectation value of the dipole operator

$$\bar{P}(t) \Rightarrow \overline{\mu(t)} \tag{11}$$

The treatment we will use for the spectroscopy is semi-classical, and follows the formalism that was popularized by Mukamel.[2] As before our Hamiltonian can generally be written as

$$H = H_0 + V(t) \tag{12}$$

where the material system is described by H_0 and treated quantum mechanically, and the electromagnetic fields $V(t)$ are treated classically and take the standard form

$$V(t) = -\bar{\mu} \cdot \bar{E} \tag{13}$$

The fields only act to drive transitions between quantum states of the system. We take the interaction with the fields to be sufficiently weak that we can treat the problem with perturbation theory. Thus, n^{th}-order perturbation theory will be used to describe the nonlinear signal derived from interacting with n electromagnetic fields.

Linear absorption spectroscopy

Absorption is the simplest example of a coherent spectroscopy. In the semi-classical picture, the polarization induced by the electromagnetic field radiates a signal field that is out-of-phase with the transmitted light. To describe this, all of the relevant information is in $R(t)$ or $\chi(\omega)$.

$$\bar{P}(t) = \int_0^\infty d\tau \, R(\tau) E(t-\tau) \tag{14}$$

$$\bar{P}(\omega) = \chi(\omega) \bar{E}(\omega) \tag{15}$$

Let's begin with a frequency-domain description of the absorption spectrum, which we previously found was proportional to the imaginary part of the susceptibility, χ''. [3] We consider one monochromatic field incident on the sample that resonantly drives dipoles in the sample to create a polarization, which subsequently re-radiate a signal field (free induction decay). For one input field, the energy and momentum conservation conditions dictate that $\omega_{in} = \omega_{sig}$ and $k_{in} = k_{sig}$, that is a signal field of the same frequency propagates in the direction of the transmitted excitation field.
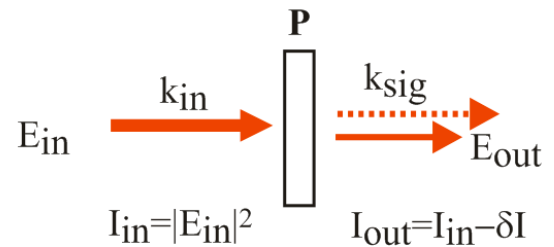
In practice, an absorption spectrum is measured by characterizing the frequency-dependent transmission decrease on adding the sample $A = -\log I_{out}/I_{in}$. For the perturbative case, let's take the change of intensity $\delta I = I_{in} - I_{out}$ to be small, so that $A \approx \delta I$ and $I_{in} \approx I_{out}$. Then we can write the measured intensity after the sample as

$$I_{out} = \left| E_{out} + E_{sig} \right|^2 = \left| E_{out} + (iP) \right|^2$$

$$= \left| E_{out} + i\chi E_{in} \right|^2 \approx \left| E_{in} + i\chi E_{in} \right|^2$$

$$= \left| E_{in} \right|^2 \left| 1 + i(\chi' + i\chi'') \right|^2 \tag{16}$$

$$= I_{in}(1 - 2\chi'' + \ldots) \qquad \Rightarrow \qquad I_{out} = I_{in} - \delta I$$

Here we have made use of the assumption that $\left| E_{in} \right| \gg \left| \chi \right|$. We see that as a result of the phase shift between the polarization and the radiated field that the absorbance is proportional to χ'':

$\delta I = 2\chi'' I_{in}$.

A time-domain approach to absorption draws on eq. (14) and should recover the relationships to the dipole autocorrelation function that we discussed previously. Equating $\overline{P}(t)$ with $\overline{\mu(t)}$, we can calculate the polarization in the density matrix picture as

$$\overline{P}(t) = Tr\left(\mu_I(t) \rho_I^{(1)}(t) \right) \tag{17}$$

where the first-order expansion of the density matrix is

$$\rho_I^{(1)} = -\frac{i}{\hbar} \int_{-\infty}^{t} dt_1 \left[V_I(t_1), \rho_{eq} \right]. \tag{18}$$

Substituting eq. (13) we find

$$\overline{P}(t) = Tr\left(\mu_I(t) \frac{i}{\hbar} \int_{-\infty}^{t} dt' \left[-\mu_I(t')E(t'), \rho_{eq} \right] \right)$$

$$= \frac{-i}{\hbar} \int_{-\infty}^{t} dt' \, E(t') \, Tr\left(\mu_I(t) \left[\mu_I(t'), \rho_{eq} \right] \right) \qquad . \tag{19}$$

$$= +\frac{i}{\hbar} \int_{0}^{\infty} d\tau \, E(t-\tau) Tr\left(\left[\mu_I(\tau), \mu_I(0) \right] \rho_{eq} \right)$$

In the last line, we switched variables to the time interval $\tau = t - t'$, and made use of the identity $\left[A, [B, C] \right] = \left[[A, B], C \right]$. Now comparing to eq. (14), we see, as expected

$$R(\tau) = \frac{i}{\hbar} \theta(\tau) Tr\left(\left[\mu_I(\tau), \mu_I(0) \right] \rho_{eq} \right) \tag{20}$$

So the linear response function is the sum of two correlation functions, or more precisely, the imaginary part of the dipole correlation function.

$$R(\tau) = \frac{i}{\hbar} \theta(\tau) \left(C(\tau) - C^*(\tau) \right) \tag{21}$$

$$C(\tau) = Tr\left(\mu_I(\tau)\mu_I(0)\rho_{eq}\right)$$
$$C^*(\tau) = Tr\left(\mu_I(\tau)\rho_{eq}\mu_I(0)\right)$$

(22)

Also, as we would expect, when we use an impulsive driving potential to induce a free induction decay (i.e., $E(t-\tau) = E_0\delta(t-\tau)$), the polarization is directly proportional to the response function, which can be Fourier transformed to obtain the absorption lineshape.

Nonlinear Polarization

For nonlinear spectroscopy, we will calculate the polarization arising from interactions with multiple fields. We will use a perturbative expansion of P in powers of the incoming fields
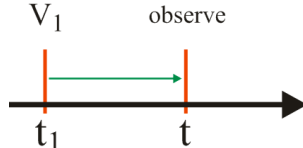
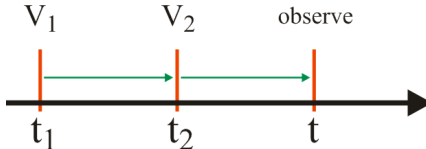$$\bar{P}(t) = P^{(0)} + P^{(1)} + P^{(2)} + P^{(3)} + \cdots$$

(23)

where $P^{(n)}$ refers to the polarization arising from n incident light fields. So, $P^{(2)}$ and higher are the nonlinear terms. We calculate P from the density matrix

$$\bar{P}(t) = Tr\left(\bar{\mu}_I(t)\rho_I(t)\right)$$
$$= Tr\left(\bar{\mu}_I\rho_I^{(0)}\right) + Tr\left(\bar{\mu}_I\,\rho_I^{(1)}(t)\right) + Tr\left(\mu_I\rho_I^{(2)}(t)\right) + \ldots$$

(24)

As we wrote earlier, $\rho_I^{(n)}$ is the nth order expansion of the density matrix

$$\rho^{(0)} = \rho_{eq}$$

$$\rho_I^{(1)} = -\frac{i}{\hbar}\int_{-\infty}^{t} dt_1\left[V_I(t_1),\rho_{eq}\right]$$

(25)

$$\rho_I^{(2)} = \left(-\frac{i}{\hbar}\right)^2\int_{-\infty}^{t} dt_2\int_{-\infty}^{t_2} dt_1\left[V_I(t_2),\left[V_I(t_1),\rho_{eq}\right]\right]$$

$$\rho_I^{(n)} = \left(-\frac{i}{\hbar}\right)^n\int_{-\infty}^{t} dt_n\int_{-\infty}^{t_n} dt_{n-1}\ldots\int_{-\infty}^{t_2} dt_1\left[V_I(t_n),\left[V_I(t_{n-1}),\left[\ldots,\left[V_I(t_1),\rho_{eq}\right]\ldots\right]\right]\right].$$

(26)

Let's examine the second-order polarization in order to describe the nonlinear response function. Earlier we stated that we could write the second-order nonlinear response arise from two time-ordered interactions with external potentials in the form

$$\overline{P}^{(2)}(t)=\int_0^\infty d\tau_2\int_0^\infty d\tau_1\; R^{(2)}(\tau_2,\tau_1)\overline{E}_1(t-\tau_2-\tau_1)\overline{E}_2(t-\tau_2) \tag{27}$$

We can compare this result to what we obtain from $P^{(2)}(t)=Tr\left(\mu_I(t)\rho_I^{(2)}(t)\right)$. Substituting as we did in the linear case,

$$
\begin{aligned}
P^{(2)}(t)&=Tr\left\{\mu_I(t)\left(-\frac{i}{\hbar}\right)^2\int_{-\infty}^t dt_2\int_{-\infty}^{t_2} dt_1\left[V_I(t_2),\left[V_I(t_1),\rho_{eq}\right]\right]\right\}\\
&=\left(\frac{i}{\hbar}\right)^2\int_{-\infty}^t dt_2\int_{-\infty}^{t_2} dt_1\, E_2(t_2)E_1(t_1)Tr\left\{\left[\left[\mu_I(t),\mu_I(t_2)\right],\mu_I(t_1)\right]\rho_{eq}\right\}\\
&=\left(\frac{i}{\hbar}\right)^2\int_0^\infty d\tau_2\int_0^\infty d\tau_1\, E_2(t-\tau_2)E_1(t-\tau_2-\tau_1)Tr\left\{\left[\left[\mu_I(\tau_1+\tau_2),\mu_I(\tau_1)\right],\mu_I(0)\right]\rho_{eq}\right\}
\end{aligned}
\tag{28}
$$

In the last line we switched variables to the time-intervals $t_1=t-\tau_1-\tau_2$ and $t_2=t-\tau_2$, and enforced the time-ordering $t_1\le t_2$. Comparison of eqs. (27) and (28) allows us to state that the second order nonlinear response function is

$$R^{(2)}(\tau_1,\tau_2)=\left(\frac{i}{\hbar}\right)^2\theta(\tau_1)\theta(\tau_2)Tr\left\{\left[\left[\mu_I(\tau_1+\tau_2),\mu_I(\tau_1)\right],\mu_I(0)\right]\rho_{eq}\right\} \tag{29}$$

Again, for impulsive interactions (i.e., delta function light pulses), the nonlinear polarization is directly proportional to the response function.

Similar exercises to the linear and second order response can be used to show that the nonlinear response function to arbitrary order $R^{(n)}$ is

$$
\begin{aligned}
R^{(n)}(\tau_1,\tau_2,\ldots\tau_n)=&\left(\frac{i}{\hbar}\right)^n\theta(\tau_1)\theta(\tau_2)\ldots\theta(\tau_n)\\
&\times Tr\left\{\left[\left[\ldots\left[\mu_I(\tau_n+\tau_{n-1}+\ldots+\tau_1),\mu_I(\tau_{n-1}+\tau_n+\cdots\tau_1)\right],\ldots\right]\mu_I(0)\right]\rho_{eq}\right\}
\end{aligned}
\tag{30}
$$

We see that in general the nonlinear response functions are sums of correlation functions, and the nth order response has 2^n correlation functions contributing. These correlation functions differ by whether sequential operators act on the *bra* or *ket* side of ρ when enforcing the time-ordering. Since the *bra* and *ket* sides represent conjugate wavefunctions, these correlation functions will contain coherences with differing phase relationships during subsequent time-intervals.

To see more specifically what a specific term in these nested commutators refers to, let's look at $R^{(2)}$ and enforce the time-ordering:

Term 1 in eq. (29):

$$Q_1 = Tr\left(\mu_I(\tau_1 + \tau_2)\mu_I(\tau_1)\mu_I(0)\rho_{eq}\right)$$

$$= Tr\left(\underline{U_0^\dagger(\tau_1 + \tau_2)}\mu\ \underline{U_0(\tau_1 + \tau_2)U_0^\dagger(\tau_1)}\ \mu\ U_0(\tau_1)\mu\ \rho_{eq}\right)$$
$$\underline{U_0^\dagger(\tau_1)U_0^\dagger(\tau_2)}\qquad \underline{U_0(\tau_2)}$$

$$= Tr\left(\mu U_0(\tau_2)\mu\ U_0(\tau_1)\mu\ \rho_{eq}U_0^\dagger(\tau_1)U_0^\dagger(\tau_2)\right)$$
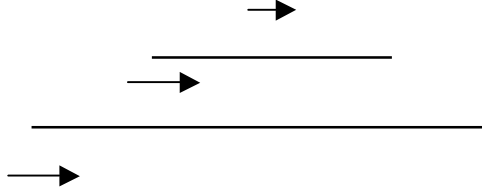
(1) dipole acts on **ket** of ρ_{eq}
(2) evolve under H_0 during τ_1.
(3) dipole acts on **ket**.
(4) Evolve during τ_2.
(5) Multiply by μ and take trace.

KET/KET interaction

At each point of interaction with the external potential, the dipole operator acted on *ket* side of ρ. Different correlation functions are distinguished by the order that they act on *bra* or *ket*. We only count the interactions with the incident fields, and the convention is that the final operator that we use prior to the trace acts on the *ket* side. So the term Q_1 is a *ket/ket* interaction.

An alternate way of expressing this correlation function is in terms of the time-propagator for the density matrix, a superoperator defined through: $\hat{G}(t)\rho_{ab} = U_0|a\rangle\langle b|U_0^\dagger$. Remembering the time-ordering, this allows Q_1 to be written as

$$Q_1 = Tr\left(\mu\hat{G}(\tau_2)\mu\hat{G}(\tau_1)\mu\rho_{eq}\right). \tag{31}$$

Term 2:

$$Q_2 = Tr\left(\mu_I(0)\mu_I(\tau_1 + \tau_2)\mu_I(\tau_1)\rho_{eq}\right)$$

$$= Tr\left(\mu_I(\tau_1 + \tau_2)\mu_I(\tau_1)\rho_{eq}\mu_I(0)\right)$$

BRA/KET interaction

For the remaining terms we note that the *bra* side interaction is the complex conjugate of *ket* side, so of the four terms in eq. (29), we can identify only two independent terms:

$$Q_1 \Rightarrow ket / ket \quad Q_1^* \Rightarrow bra / bra \quad Q_2 \Rightarrow ket / bra \quad Q_2^* = bra / ket.$$

This is a general observation. For $R^{(n)}$, you really only need to calculate 2^{n-1} correlation functions. So for $R^{(2)}$ we write

$$R^{(2)} = \left(\frac{i}{\hbar}\right)^2 \theta(\tau_1)\theta(\tau_2) \sum_{\alpha=1}^{2} \left[Q_\alpha(\tau_1,\tau_2) - Q_\alpha^*(\tau_1,\tau_2)\right] \tag{32}$$

where

$$Q_1 = Tr\left[\mu_I(\tau_1+\tau_2)\mu_I(\tau_1)\mu_I(0)\rho_{eq}\right] \tag{33}$$

$$Q_2 = Tr\left[\mu_I(\tau_1)\mu_I(\tau_1+\tau_2)\mu_I(0)\rho_{eq}\right]. \tag{34}$$

So what is the difference in these correlation functions? Once there is more than one excitation field, and more than one time period during which coherences can evolve, then one must start to carefully watch the relative phase that coherences acquire during different consecutive time-periods, $\phi(\tau) = \omega_{ab}\tau$. To illustrate, consider wavepacket evolution: light interaction can impart positive or negative momentum ($\pm \overline{k}_{in}$) to the evolution of the wavepacket, which influences the direction of propagation and the phase of motion relative to other states. Any subsequent field that acts on this state must account for time-dependent overlap of these wavepackets with other target states. The different terms in the nonlinear response function account for all of the permutations of interactions and the phase acquired by these coherences involved. The sum describes the evolution including possible interference effects between different interaction pathways.

Third-Order Response

Since $R^{(2)}$ orientationally averages to zero for isotropic systems, the third-order nonlinear response described the most widely used class of nonlinear spectroscopies.

$$R^{(3)}(\tau_1,\tau_2,\tau_3) = \left(\frac{i}{\hbar}\right)^3 \theta(\tau_3)\theta(\tau_2)\theta(\tau_1) Tr\left\{\left[\left[\left[\mu_I(\tau_1+\tau_2+\tau_3),\mu_I(\tau_1+\tau_2)\right],\mu_I(\tau_1)\right],\mu_I(0)\right]\rho_{eq}\right\} \tag{35}$$

$$R^{(3)}(\tau_1,\tau_2,\tau_3)=\left(\frac{i}{\hbar}\right)^3\theta(\tau_3)\theta(\tau_2)\theta(\tau_1)\sum_{\alpha=1}^{4}\left[R_\alpha(\tau_3,\tau_2,\tau_1)-R_\alpha^*(\tau_3,\tau_2,\tau_1)\right] \tag{36}$$

Here the convention for the time-ordered interactions with the density matrix is $R_1 = ket\,/\,ket\,/\,ket$; $R_2 = bra\,/\,ket\,/\,bra$; $R_3 = bra\,/\,bra\,/\,ket$; and $R_4 \Rightarrow ket\,/\,bra\,/\,bra$. In the eigenstate representation, the individual correlation functions can be explicitly written in terms of a sum over all possible intermediate states (a,b,c,d):

$$R_1 = \sum_{a,b,c,d} p_a \left\langle \mu_{ad}(\tau_1+\tau_2+\tau_3)\mu_{dc}(\tau_1+\tau_2)\mu_{cb}(\tau_1)\mu_{ba}(0)\right\rangle$$

$$R_2 = \sum_{a,b,c,d} p_a \left\langle \mu_{ad}(0)\mu_{dc}(\tau_1+\tau_2)\mu_{cb}(\tau_1+\tau_2+\tau_3)\mu_{ba}(\tau_1)\right\rangle$$

$$\tag{37}$$

$$R_3 = \sum_{a,b,c,d} p_a \left\langle \mu_{ad}(0)\mu_{dc}(\tau_1)\mu_{cb}(\tau_1+\tau_2+\tau_3)\mu_{ba}(\tau_1+\tau_2)\right\rangle$$

$$R_4 = \sum_{a,b,c,d} p_a \left\langle \mu_{ad}(\tau_1)\mu_{dc}(\tau_1+\tau_2)\mu_{cb}(\tau_1+\tau_2+\tau_3)\mu_{ba}(0)\right\rangle$$

## Summary: General Expressions for n^{th} Order Nonlinearity

For an nth-order nonlinear signal, there are n interactions with the incident electric field or fields that give rise to the radiated signal. Counting the radiated signal there are $n+1$ fields involved ($n+1$ light-matter interactions), so that n^{th} order spectroscopy is at times referred to as $(n+1)$-wave mixing.

The radiated nonlinear signal field is proportional to the nonlinear polarization:

$$P^{(n)}(t)=\int_0^\infty d\tau_n\cdots\int_0^\infty d\tau_1\, R^{(n)}(\tau_1,\tau_2,\dots\tau_n)\bar{E}_1(t-\tau_n-\cdots-\tau_1)\cdots\bar{E}_n(t-\tau_n) \tag{38}$$

$$R^{(n)}(\tau_1,\tau_2,\dots\tau_n)=\left(\frac{i}{\hbar}\right)^n\theta(\tau_1)\theta(\tau_2)\dots\theta(\tau_n)$$
$$\times Tr\left\{\left[\left[\dots\left[\mu_I(\tau_n+\tau_{n-1}+\dots+\tau_1),\mu_I(\tau_{n-1}+\tau_n+\cdots\tau_1)\right],\dots\right]\mu_I(0)\right]\rho_{eq}\right\} \tag{39}$$

Here the interactions of the light and matter are expressed in terms of a sequence of consecutive time-intervals $\tau_1\dots\tau_n$ prior to observing
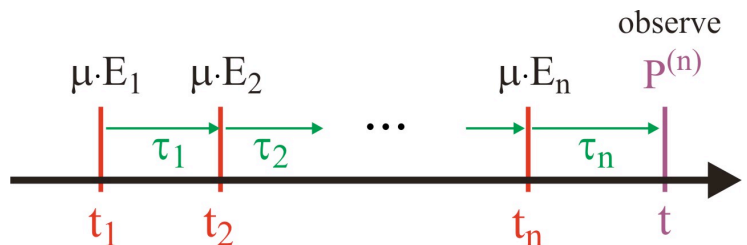
the system. For delta-function interactions, $\bar{E}_i(t-t_0)=\left|\bar{E}_i\right|\delta(t-t_0)$, the polarization and response function are directly proportional

$$P^{(n)}(t)=R^{(n)}(\tau_1,\tau_2,\ldots\tau_{n-1},t)\left|\bar{E}_1\right|\cdots\left|\bar{E}_n\right|. \tag{40}$$

---

1. The radiation pattern in the far field for the electric field emitted by a dipole aligned along the z axis is

$$E(r,\theta,\phi,t)=-\frac{p_0 k^2}{4\pi\varepsilon_0}\frac{\sin\theta}{r}\sin(k\cdot r-\omega t).$$

   (written in spherical coordinates). See Jackson, *Classical Electrodynamics*.

2. S. Mukamel, *Principles of Nonlinear Optical Spectroscopy*. (Oxford University Press, New York, 1995).

3. Remember the following relationships of the susceptibility with the complex dielectric constant $\varepsilon(\omega)$, the index of refraction $n(\omega)$, and the absorption coefficient $\kappa(\omega)$:

$$\varepsilon(\omega)=1+4\pi\chi(\omega)$$

$$\sqrt{\varepsilon(\omega)}=\tilde{n}(\omega)=n(\omega)+i\kappa(\omega)$$

3. **Diagrammatic Perturbation Theory**

In practice, the nonlinear response functions as written above provide little insight into what the molecular origin of particular nonlinear signals is. These multiply nested terms are difficult to understand when faced the numerous light-matter interactions, which can take on huge range of permutations when performing experiments on a system with multiple quantum states. The different terms in the response function can lead to an array of different nonlinear signals that vary not only microscopically by the time-evolution of the molecular system, but also differ macroscopically in terms of the frequency and wavevector of the emitted radiation.

Diagrammatic perturbation theory (DPT) is a simplified way of keeping track of the contributions to a particular nonlinear signal given a particular set of states in H_0 that are probed in an experiment. It uses a series of simple diagrams to represent the evolution of the density matrix for H_0, showing repeated interaction of ρ with the fields followed by time-propagation under H_0. From a practical sense, DPT allows us to interpret the microscopic origin of a signal with a particular frequency and wavevector of detection, given the specifics of the quantum system we are studying and the details of the incident radiation. It provides a shorthand form of the correlation functions contributing to a particular nonlinear signal, which can be used to understand the microscopic information content of particular experiments. It is also a bookkeeping method that allows us to keep track of the contributions of the incident fields to the frequency and wavevector of the nonlinear polarization.

There are two types of diagrams we will discuss, Feynman and ladder diagrams, each of which has certain advantages and disadvantages. For both types of diagrams, the first step in drawing a diagram is to identify the states of H_0 that will be interrogated by the light-fields. The diagrams show an explicit series of absorption or stimulated emission events induced by the incident fields which appear as action of the dipole operator on the *bra* or *ket* side of the density matrix. They also symbolize the coherence or population state in which the density matrix evolves during a given time interval. The trace taken at the end following the action of the final dipole operator, i.e. the signal emission, is represented by a final wavy line connecting dipole coupled states.

Feynman Diagrams

Feynman diagrams are the easiest way of tracking the state of coherences in different time periods, and for noting absorption and emission events.

1. Double line represents *ket* and *bra* side of ρ.

2. Time-evolution is upward.

3. Lines intersecting diagram represent field interaction. Absorption is designated through an inward pointing arrow. Emission is an outward pointing arrow. Action on the left line is action on the *ket*, whereas the right line is *bra*.

4. System evolves freely under H_0 between interactions, and density matrix element for that period is often explicitly written.
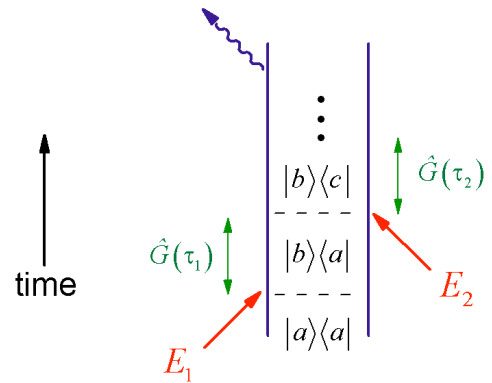
Ladder Diagrams[1]

Ladder diagrams are helpful for describing experiments on multistate systems and/or with multiple frequencies; however, it is difficult to immediately see the state of the system during a given time interval. They naturally lend themselves to a description of interactions in terms of the eigenstates of H_0.

1. Multiple states arranged vertically by energy.

2. Time propagates to right.

3. Arrows connecting levels indicate resonant interactions. Absorption is an upward arrow and emission is downward. A solid line is used to indicate action on the *ket*, whereas a dotted line is action on the *bra*.

4. Free propagation under H_0 between interactions, but the state of the density matrix is not always obvious.
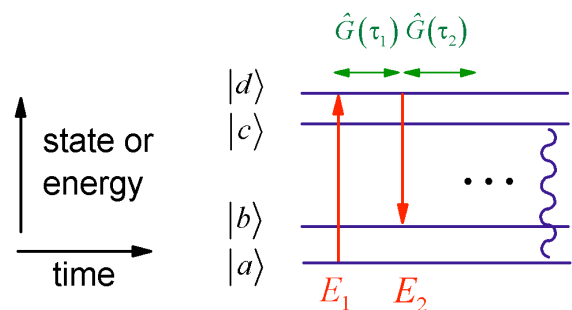
For each light-matter interactions represented in a diagram, there is an understanding of how this action contributes to the response function and the final nonlinear polarization state. Each light-matter interaction acts on one side of ρ, either through absorption or stimulated emission. Each interaction adds a dipole matrix element μ_{ij} that describes the interaction amplitude and any orientational effects.[2] Each interaction adds input electric field factors to the polarization, which are used to describe the frequency and wavevector of the radiated signal. The action of the final dipole operator must return you to a diagonal element to contribute to the signal. Remember that action on the *bra* is the complex conjugate of *ket* and absorption is complex conjugate of stimulated emission. A table summarizing these interactions contributing to a diagram is below.

Interaction	Diagrammatic Representation	contrib. to $R^{(n)}$	contribution to $\mathbf{k}_{sig}$ & ω_{sig}	
KET SIDE				
Absorption $\left(\bar{\mu}_{ba} \cdot \bar{E}_n\right)\exp\left[i\bar{k}_n \cdot \bar{r} - i\omega_n t\right]$		$\bar{\mu}_{ba} \cdot \hat{\varepsilon}_n$	$+\mathbf{k_n}$	$+\omega_n$
Stimulated Emission $\left(\bar{\mu}_{ba} \cdot \bar{E}_n^*\right)\exp\left[-i\bar{k}_n \cdot \bar{r} + i\omega_n t\right]$		$\bar{\mu}_{ba} \cdot \hat{\varepsilon}_n$	$-\mathbf{k_n}$	$-\omega_n$
BRA SIDE				
Absorption $\left(\bar{\mu}_{ba}^* \cdot \bar{E}_n^*\right)exp\left[-i\bar{k}_n \cdot \bar{r} + i\omega_n t\right]$		$\bar{\mu}_{ba}^* \cdot \hat{\varepsilon}_n$	$-\mathbf{k_n}$	$-\omega_n$
Stimulated Emission $\left(\bar{\mu}_{ba}^* \cdot \bar{E}_n\right)exp\left[i\bar{k}_n \cdot \bar{r} - i\omega_n t\right]$		$\bar{\mu}_{ba}^* \cdot \hat{\varepsilon}_n$	$+\mathbf{k_n}$	$+\omega_n$
SIGNAL EMISSION: (Final trace, convention: ket side)		$\bar{\mu}_{ba} \cdot \hat{\varepsilon}_{an}$		

Once you have written down the relevant diagrams, being careful to identify all permutations of interactions of your system states with the fields relevant to your signal, the correlation functions contributing to the material response and the frequency and wavevector of the signal field can be readily obtained. It is convenient to write the correlation function as a product of several factors for each event during the series of interactions:

1) Start with a factor p_n signifying the probability of occupying the initial state, typically a Boltzmann factor.

2) Read off products of transition dipole moments for interactions with the incident fields, and for the final signal emission.

3) Multiply by terms that describe the propagation under H_0 between interactions.

   As a starting point for understanding an experiment, it is valuable to include the effects of relaxation of the system eigenstates in the time-evolution using a simple phenomenological approach. Coherences and populations are propagated by assigning the damping constant Γ_{ab} to propagation of the ρ_{ab} element:

   $$\hat{G}(\tau)\rho_{ab} = \exp\left[-i\omega_{ab}\tau - \Gamma_{ab}\tau\right]\rho_{ab}. \tag{41}$$

   Note $\Gamma_{ab} = \Gamma_{ba}$ and $G_{ab}^* = G_{ba}$. We can then recognize $\Gamma_{ii} = 1/T_1$ as the population relaxation rate for state i and $\Gamma_{ij} = 1/T_2$ the dephasing rate for the coherence ρ_{ij}.
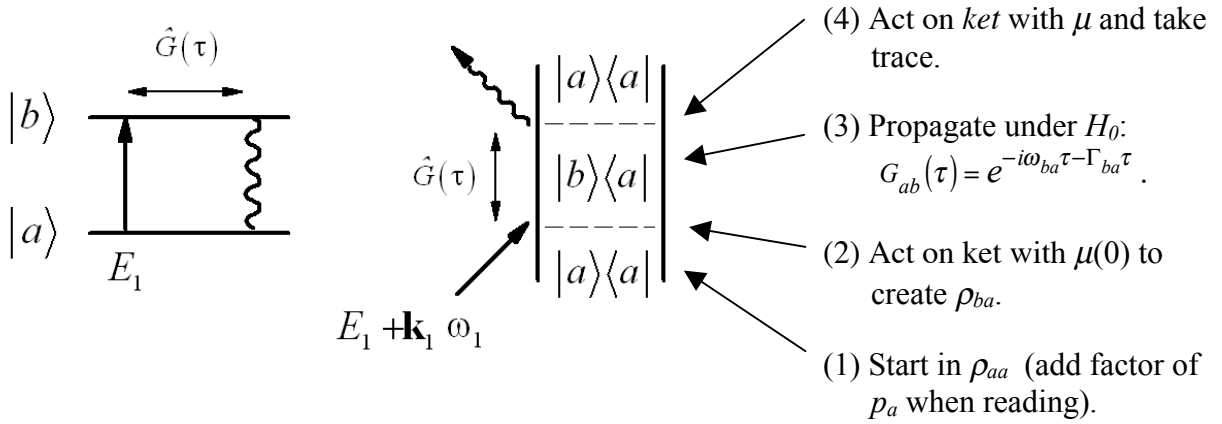
4) Multiply by a factor of $(-1)^n$ where n is the number of *bra* side interactions. This factor accounts for the fact that in evaluating the nested commutator, some correlation functions are subtracted from others.

5) The radiated signal will have frequency $\omega_{sig} = \sum_i \omega_i$ and wave vector $\bar{k}_{sig} = \sum_i \bar{k}_i$

Example: Linear Response for a Two-Level System

Let's consider the diagrammatic approach to the linear absorption problem, using a two-level system with a lower level a and upper level b. There is only one independent correlation function in the linear response function,

$$C(t) = Tr\left[\mu(t)\mu(0)\rho_{eq}\right]$$
$$= Tr\left[\mu\,\hat{G}(t)\mu\rho_{eq}\right] \tag{42}$$

This does not need to be known before starting, but is useful to consider, since it should be recovered in the end. The system will be taken to start in the ground state ρ_{aa}. Linear response only allows for one input field interaction, which must be absorption, and which we take to be a *ket* side interaction. We can now draw two diagrams:

(4) Act on *ket* with μ and take trace.

(3) Propagate under H_0:
$$G_{ab}(\tau) = e^{-i\omega_{ba}\tau - \Gamma_{ba}\tau}.$$

(2) Act on ket with $\mu(0)$ to create ρ_{ba}.

(1) Start in ρ_{aa} (add factor of p_a when reading).

With this diagram, we can begin by describing the signal characteristics in terms of the induced polarization. The product of incident fields indicates:

$$E_1 e^{-i\omega_1 t + i\bar{k}_1 \cdot \bar{r}} \quad \Rightarrow \quad P(t) e^{-i\omega_{sig} t + i\bar{k}_{sig} \cdot \bar{r}} \tag{43}$$

so that
$$\omega_{sig} = \omega_1 \quad \bar{k}_{sig} = \bar{k} . \tag{44}$$

As expected the signal will radiate with the same frequency and in the same direction as the incoming beam. Next we can write down the correlation function for this term. Working from bottom up:

$$\overset{(1)\,(2)}{} \quad \overset{(3)}{} \quad \overset{(4)}{}$$
$$C(t) = p_a\left[\mu_{ba}\right]\left[e^{-i\omega_{ba}t - \Gamma_{ba}t}\right]\left[\mu_{ab}\right] \tag{45}$$
$$= p_a\left|\mu_{ba}\right|^2 e^{-i\omega_{ba}t - \Gamma_{ba}t}$$

More sophisticated ways of treating the time-evolution under H_0 in step (*3*) could take the form of some of our earlier treatments of the absorption lineshape:

$$\hat{G}(\tau)\rho_{ab} \sim \rho_{ab}\exp\left[-i\omega_{ab}\tau\right]F(\tau)$$
$$= \rho_{ab}\exp\left[-i\omega_{ab}\tau - g(t)\right]$$

(46)

Note that one could draw four possible permutations of the linear diagram when considering *bra* and *ket* side interactions, and initial population in states *a* and *b*:
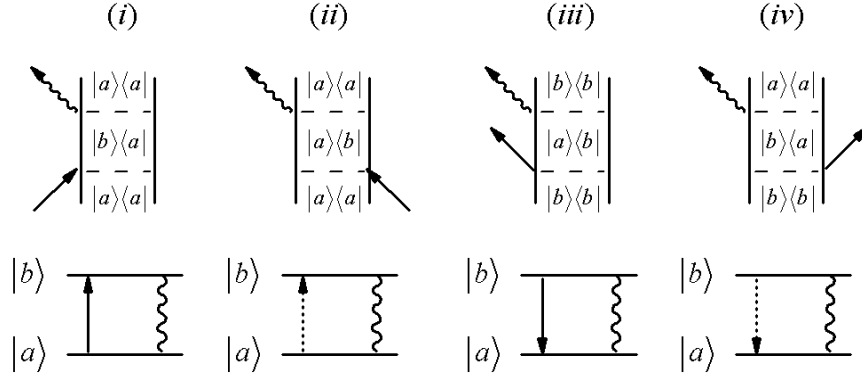
However, there is no new dynamical content in these extra diagrams, and they are generally taken to be understood through one diagram. Diagram *ii* is just the complex conjugate of eq. (45) so adding this signal contribution gives:
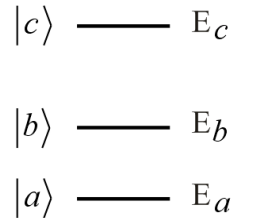
$$C(t) - C^*(t) = 2i\, p_a\left|\mu_{ba}\right|^2 \sin(\omega_{ba}t)e^{-\Gamma_{ba}t}.$$
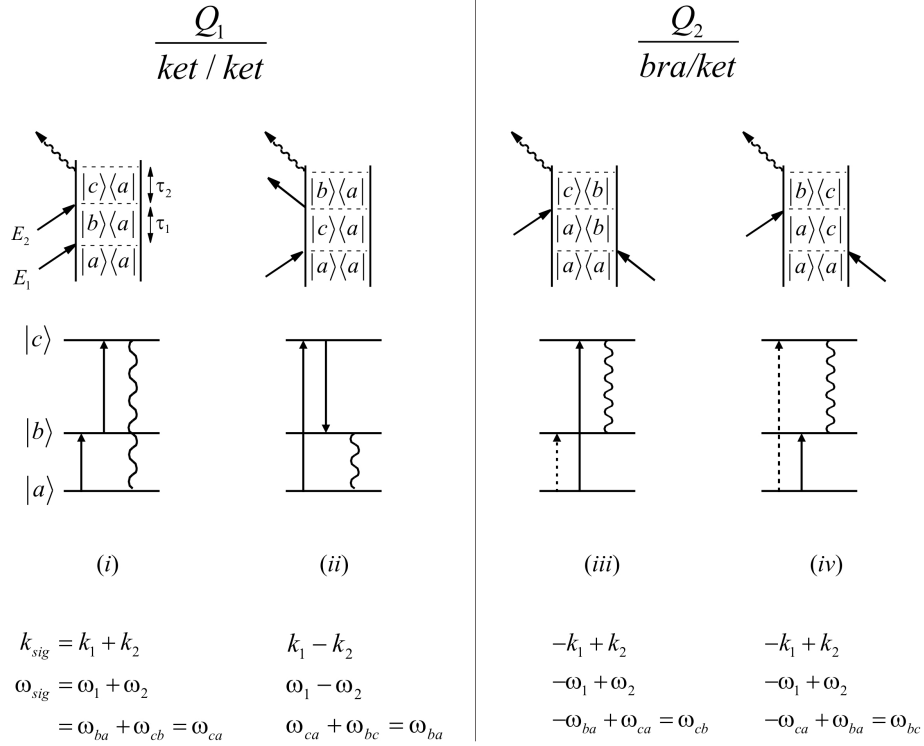
(47)

Accounting for the thermally excited population initially in *b* leads to the expected two-level system response function that depends on the population difference

$$R(t) = \frac{2}{\hbar}(p_a - p_b)\left|\mu_{ba}\right|^2 \sin(\omega_{ba}t)e^{-\Gamma_{ba}t}.$$

(48)

Example: Second-Order Response for a Three-Level System

The second-order response is the simplest nonlinear case, but in molecular spectroscopy is less commonly used than third-order measurements. The signal generation requires a lack of inversion symmetry, which makes it useful for studies of interfaces and chiral systems. However, let's show how one would diagrammatically evaluate the second order response for a very specific system pictured at right. If we only have population in the ground state at equilibrium and if there are only resonant interactions allowed, the permutations of unique diagrams are as follows:

$$|c\rangle \ \rule{2em}{0.4pt}\ \mathrm{E}_c$$

$$|b\rangle \ \rule{2em}{0.4pt}\ \mathrm{E}_b$$

$$|a\rangle \ \rule{2em}{0.4pt}\ \mathrm{E}_a$$

$$\frac{Q_1}{ket \, / \, ket}$$ $$\frac{Q_2}{bra/ket}$$

$$k_{sig} = k_1 + k_2 \qquad\qquad k_1 - k_2 \qquad\qquad -k_1 + k_2 \qquad\qquad -k_1 + k_2$$
$$\omega_{sig} = \omega_1 + \omega_2 \qquad\qquad \omega_1 - \omega_2 \qquad\qquad -\omega_1 + \omega_2 \qquad\qquad -\omega_1 + \omega_2$$
$$= \omega_{ba} + \omega_{cb} = \omega_{ca} \qquad \omega_{ca} + \omega_{bc} = \omega_{ba} \qquad -\omega_{ba} + \omega_{ca} = \omega_{cb} \qquad -\omega_{ca} + \omega_{ba} = \omega_{bc}$$

From the frequency conservation conditions, it should be clear that process *i* is a sum-frequency signal for the incident fields, whereas diagrams *ii-iv* refer to difference frequency schemes. To better interpret what these diagrams refer to let's look at *iii*. Reading in a time-ordered manner, we can write the correlation function corresponding to this diagram as

$$C_2 = Tr\left[\mu(\tau)\rho_{eq}\mu(0)\right]$$
$$= (-1)^1 \, \mu_{bc} \, \hat{G}_{cb}(\tau_2) \mu_{ca} \, \hat{G}_{ab}(\tau_1) \, \rho_{aa} \, \mu_{ba}^* \, . \tag{49}$$
$$= -p_a \mu_{ab}\mu_{bc}\mu_{ca} e^{-i\omega_{ab}\tau_1 - \Gamma_{ab}\tau_1} e^{-i\omega_{cb}\tau_2 - \Gamma_{cb}\tau_2}$$

Note that a literal interpretation of the final trace in diagram *iv* would imply an absorption event – an upward transition from *b* to *c*. What does this have to do with radiating a signal? On the one hand it is important to remember that a diagram is just mathematical shorthand, and that one can't distinguish absorption and emission in the final action of the dipole operator prior to taking a trace. The other thing to remember is that such a diagram always has a complex conjugate associated with it in the response function. The complex conjugate of *iv*, a Q_2^* *ket/bra* term,

$$\frac{Q_2^*}{ket/bra}$$

$(iv)^*$
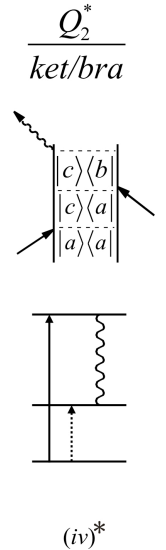
shown at right has a downward transition –emission– as the final interaction. The combination $Q_2 - Q_2^*$ ultimately describes the observable.

Now, consider the wavevector matching conditions for the second order signal *iii*. Remembering that the magnitude of the wavevector is $|\bar{k}| = \omega/c = 2\pi/\lambda$, the length of the vectors will be scaled by the resonance frequencies. When the two incident fields are crossed as a slight angle, the signal would be phase-matched such that the signal is radiated closest to beam 2. Note that the most efficient wavevector matching here would be when fields 1 and 2 are collinear.
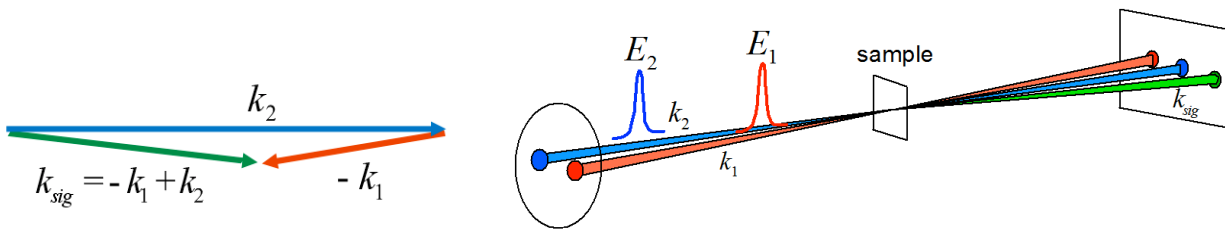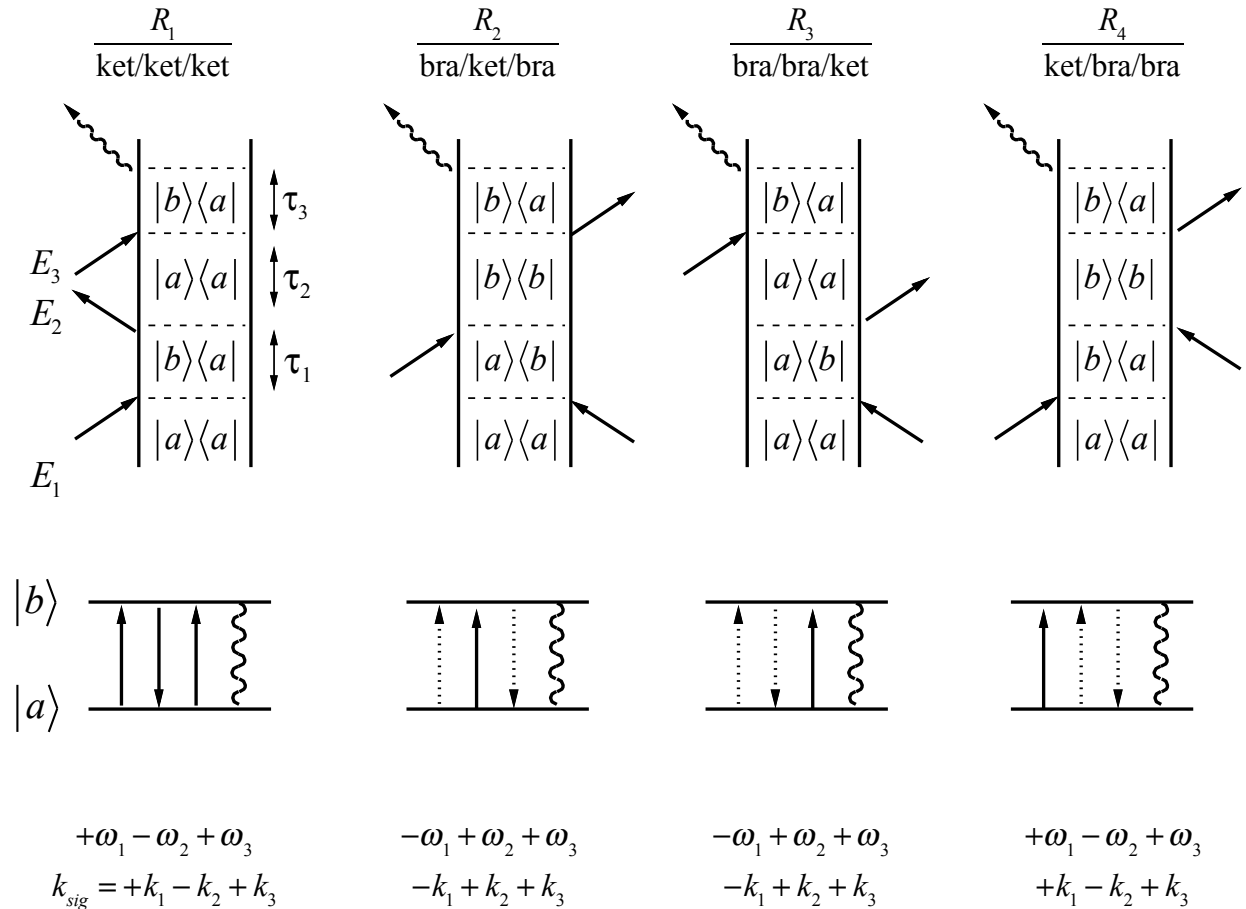
Third-Order Nonlinear Spectroscopy

Now let's look at examples of diagrammatic perturbation theory applied to third-order nonlinear spectroscopy. Third-order nonlinearities describe the majority of coherent nonlinear experiments that are used including pump-probe experiments, transient gratings, photon echoes, coherent anti-Stokes Raman spectroscopy (CARS), and degenerate four wave mixing (4WM). These experiments are described by some or all of the eight correlation functions contributing to $R^{(3)}$:

$$R^{(3)} = \left(\frac{i}{\hbar}\right)^3 \sum_{\alpha=1}^{4} \left[R_\alpha - R_\alpha^*\right] \tag{50}$$

The diagrams and corresponding response first requires that we specify the system eigenstates. The simplest case, which allows us discuss a number of examples of third-order spectroscopy is a two-level system. Let's write out the diagrams and correlation functions for a two-level system starting in ρ_{aa}, where the dipole operator couples $|b\rangle$ and $|a\rangle$.

| $\dfrac{R_1}{\text{ket/ket/ket}}$ | $\dfrac{R_2}{\text{bra/ket/bra}}$ | $\dfrac{R_3}{\text{bra/bra/ket}}$ | $\dfrac{R_4}{\text{ket/bra/bra}}$ |

$$+\omega_1 - \omega_2 + \omega_3$$
$$k_{sig} = +k_1 - k_2 + k_3$$

$$-\omega_1 + \omega_2 + \omega_3$$
$$-k_1 + k_2 + k_3$$

$$-\omega_1 + \omega_2 + \omega_3$$
$$-k_1 + k_2 + k_3$$

$$+\omega_1 - \omega_2 + \omega_3$$
$$+k_1 - k_2 + k_3$$

As an example, let's write out the correlation function for R_2 obtained from the diagram above. This term is important for understanding photon echo experiments and contributes to pump-probe and degenerate four-wave mixing experiments.

$$R_2 = (-1)^2 p_a \left(\mu_{ba}^* \right) \left[e^{-i\omega_{ab}\tau_1 - \Gamma_{ab}\tau_1} \right] \left(\mu_{ba} \right) \left(e^{-i\omega_{bb}\tau_2 - \Gamma_{bb}\tau_2} \right) \left(\mu_{ab}^* \right) \left[e^{-i\omega_{ba}\tau_3 - \Gamma_{ba}\tau_3} \right] \left(\mu_{ab} \right)$$
$$= p_a |\mu_{ab}|^4 \exp\left[-i\omega_{ba}(\tau_3 - \tau_1) - \Gamma_{ba}(\tau_1 + \tau_3) - \Gamma_{bb}(\tau_2) \right] \tag{51}$$

The diagrams show how the input field contributions dictate the signal field frequency and wave-vector. Recognizing the dependence of $E_{sig}^{(3)} \sim P^{(3)} \sim R_2(E_1 E_2 E_3)$, these are obtained from the product of the incident field contributions

$$\bar{E}_1 \bar{E}_2 \bar{E}_3 = \left(E_1^* e^{+i\omega_1 t - i\bar{k}_1 \cdot \bar{r}} \right) \left(E_2 e^{-i\omega_2 t + i\bar{k}_2 \cdot r} \right) \left(E_3 e^{+i\omega_3 t - i\bar{k}_3 \cdot \bar{r}} \right)$$
$$\Rightarrow E_1^* E_2 E_3 e^{-\omega_{sig} t + i\bar{k}_{sig} \cdot \bar{r}} \tag{52}$$

$$\therefore \; \omega_{sig2} = -\omega_1 + \omega_2 + \omega_3$$
$$k_{sig2} = -\bar{k}_1 + \bar{k}_2 + \bar{k}_3 \tag{53}$$

Now, let's compare this to the response obtained from R_4. These we obtain

$$R_4 = p_a |\mu_{ab}|^4 \exp\left[-i\omega_{ba}(\tau_3 + \tau_1) - \Gamma_{ba}(\tau_1 + \tau_3) - \Gamma_{bb}(\tau_2) \right] \tag{54}$$

$$\omega_{sig4} = +\omega_1 - \omega_2 + \omega_3$$
$$k_{sig4} = +\bar{k}_1 - \bar{k}_2 + \bar{k}_3 \tag{55}$$

Note that R_2 and R_4 terms are identical, except for the phase acquired during the initial period: $\exp[i\phi] = \exp[\pm i\omega_{ba}\tau_1]$. The R_2 term evolves in conjugate coherences during the τ_1 and τ_3 periods, whereas the R_4 term evolves in the same coherence state during both periods:

	Coherences in τ_1 and τ_3	Phase acquired in τ_1 and τ_3
R_4	$|b\rangle\langle a| \to |b\rangle\langle a|$	$e^{-i\omega_{ba}(\tau_1 + \tau_3)}$
R_2	$|a\rangle\langle b| \to |b\rangle\langle a|$	$e^{-i\omega_{ba}(\tau_1 - \tau_3)}$

The R_2 term has the property of time-reversal: the phase acquired during τ_1 is reversed in τ_3. For that reason the term is called "rephasing." Rephasing signals are selected in photon echo experiments and are used to distinguish line broadening mechanisms and study spectral

diffusion. For R_4, the phase acquired continuously in τ_1 and τ_3, and this term is called "non-rephasing." Analysis of R_1 and R_3 reveals that these terms are non-rephasing and rephasing, respectively.
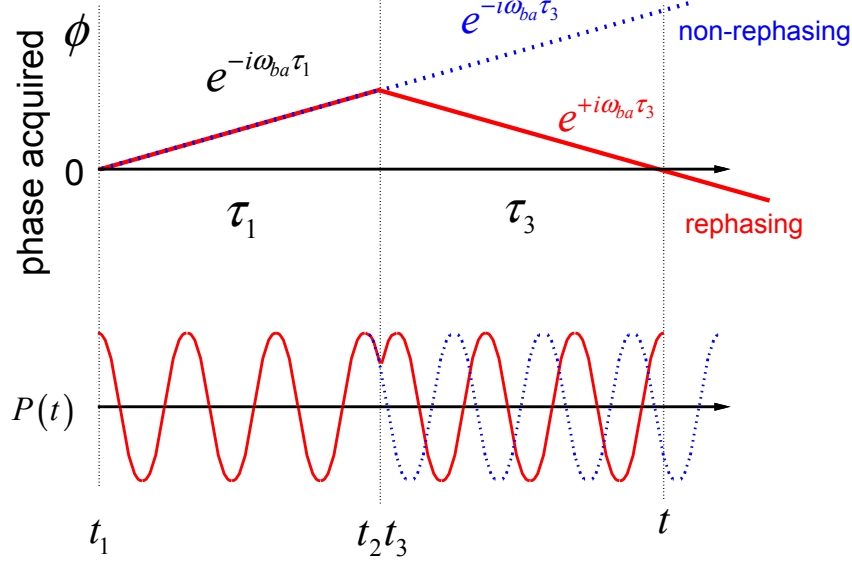
For the present case of a third-order spectroscopy applied to a two-level system, we observe that the two rephasing functions R_2 and R_3 have the same emission frequency and wavevector, and would therefore both contribute equally to a given detection geometry. The two terms differ in which population state they propagate during the τ_2 variable. Similarly, the non-rephasing functions R_1 and R_4 each have the same emission frequency and wavevector, but differ by the τ_2 population. For transitions between more than two system states, these terms could be separated by frequency or wavevector (see appendix). Since the rephasing pair R_2 and R_3 both contribute equally to a signal scattered in the $-k_1 + k_2 + k_3$ direction, they are also referred to as S_I. The nonrephasing pair R_1 and R_4 both scatter in the $+k_1 - k_2 + k_3$ direction and are labeled as S_II.

Our findings for the four independent correlation functions are summarized below.

			ω_{sig}	k_{sig}	τ_2 population
S_I	rephasing	R_2	$-\omega_1 + \omega_2 + \omega_3$	$-k_1 + k_2 + k_3$	excited state
		R_3	$-\omega_1 + \omega_2 + \omega_3$	$-k_1 + k_2 + k_3$	ground state
S_II	non-rephasing	R_1	$+\omega_1 - \omega_2 + \omega_3$	$+k_1 - k_2 + k_3$	ground state
		R_4	$+\omega_1 - \omega_2 + \omega_3$	$+k_1 - k_2 + k_3$	excited state

Frequency Domain Representation[3]

A Fourier-Laplace transform of $P^{(3)}(t)$ with respect to the time intervals allows us to obtain an expression for the third order nonlinear susceptibility, $\chi^{(3)}(\omega_1, \omega_2, \omega_3)$:

$$P^{(3)}(\omega_{sig}) = \chi^{(3)}(\omega_{sig}; \omega_1, \omega_2, \omega_3) \bar{E}_1 \bar{E}_2 \bar{E}_3 \qquad (56)$$

where

$$\chi^{(n)} = \int_0^\infty d\tau_n e^{i\Omega_n \tau_n} \cdots \int_0^\infty d\tau_1 e^{i\Omega_1 \tau_1} R^{(n)}(\tau_1, \tau_2, \ldots \tau_n) . \qquad (57)$$

Here the Fourier transform conjugate variables Ω_m to the time-interval τ_m are the sum over all frequencies for the incident field interactions up to the period for which you are evolving:

$$\Omega_m = \sum_{i=1}^m \omega_i \qquad (58)$$

For instance, the conjugate variable for the third time-interval of a $+k_1 - k_2 + k_3$ experiment is the sum over the three preceding incident frequencies $\Omega_3 = \omega_1 - \omega_2 + \omega_3$.

In general, $\chi^{(3)}$ is a sum over many correlation functions and includes a sum over states:

$$\chi^{(3)}(\omega_1, \omega_2, \omega_3) = \frac{1}{6} \left(\frac{i}{\hbar} \right)^3 \sum_{abcd} p_a \sum_{\alpha=1}^4 \left[\chi_\alpha - \chi_\alpha^* \right] \qquad (59)$$

Here a is the initial state and the sum is over all possible intermediate states. Also, to describe frequency domain experiments, we have to permute over all possible time orderings. Most generally, the eight terms in $R^{(3)}$ lead to 48 terms for $\chi^{(3)}$, as a result of the 3!=6 permutations of the time-ordering of the input fields.[4]

Given a set of diagrams, we can write the nonlinear susceptibility directly as follows:

1)   Read off products of light-matter interaction factors.

2)   Multiply by resonance denominator terms that describe the propagation under H_0. In the frequency domain, if we apply eq. (57) to response functions that use phenomenological time-propagators of the form eq. (41), we obtain

$$\hat{G}(\tau_m)\rho_{ab} \implies \frac{1}{(\Omega_m - \omega_{ba}) - i\Gamma_{ba}} . \qquad (60)$$

Ω_m is defined in eq. (58).

3)   As for the time domain, multiply by a factor of $(-1)^n$ for n *bra* side interactions.

4)   The radiated signal will have frequency $\omega_{sig} = \sum_i \omega_i$ and wavevector $\overline{k}_{sig} = \sum_i \overline{k}_i$.
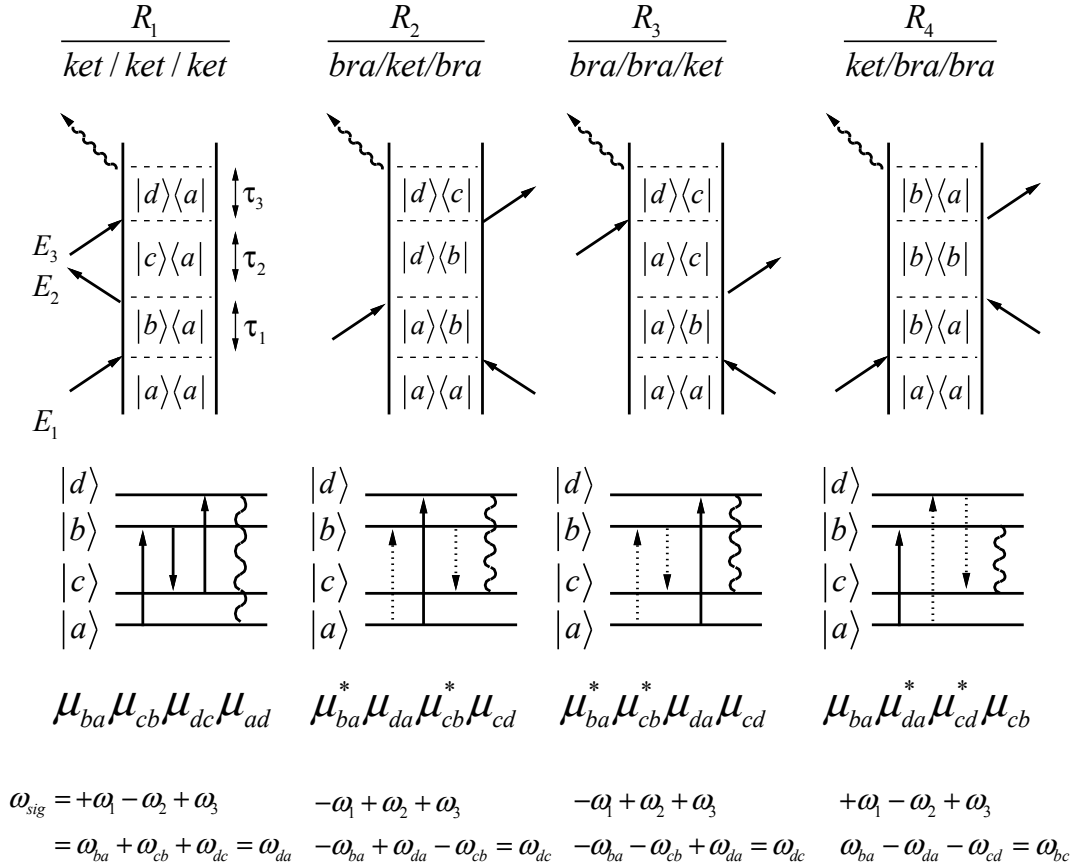
As an example, consider the term for R_2 applied to a two-level system that we wrote in the time domain in eq. (51)

$$
\begin{aligned}
\chi_2 &= \left|\mu_{ba}\right|^4 \frac{(-1)}{\omega_{ab}-(-\omega_1)-i\Gamma_{ab}} \cdot \frac{1}{\omega_{bb}-(\omega_2-\omega_1)-i\Gamma_{bb}} \cdot \frac{(-1)}{\omega_{ba}-(\omega_3+\omega_2-\omega_1)-i\Gamma_{ba}} \\
&= \left|\mu_{ba}\right|^4 \frac{1}{\omega_1-\omega_{ba}-i\Gamma_{ba}} \cdot \frac{1}{-(\omega_2-\omega_1)-i\Gamma_{bb}} \cdot \frac{1}{-(\omega_3+\omega_2-\omega_1-\omega_{ba})-i\Gamma_{ba}}
\end{aligned}
$$

(61)

The terms are written from a diagram with each interaction and propagation adding a resonant denominator term (here reading left to right). The full frequency domain response is a sum over multiple terms like these.

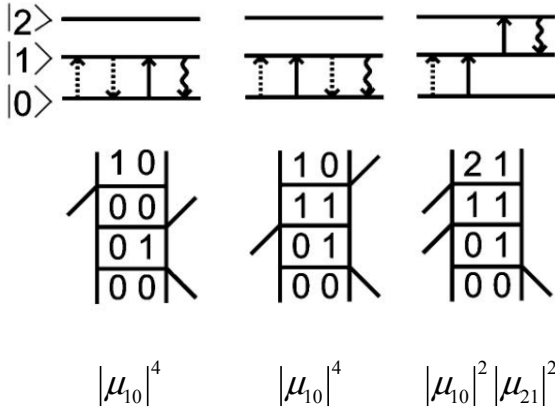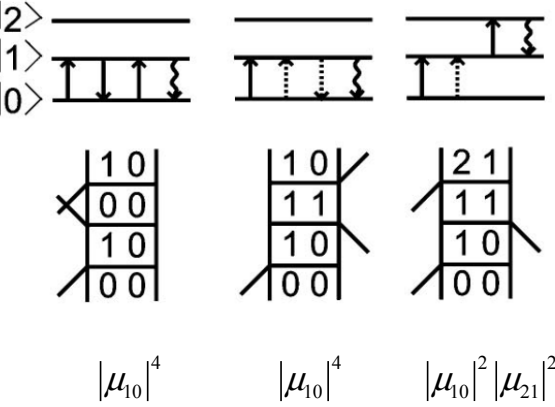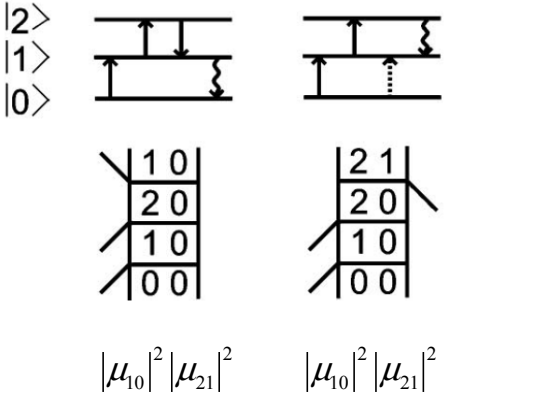## Appendix: Third-order diagrams for a four-level system

The third order response function can describe interaction with up to four eigenstates of the system Hamiltonian. These are examples of correlation functions within $R^{(3)}$ for a four-level system representative of vibronic transitions accompanying an electronic excitation, as relevant to resonance Raman spectroscopy. Note that these diagrams present only one example of multiple permutations that must be considered given a particular time-sequence of incident fields that may have variable frequency.

R_1	R_2	R_3	R_4
ket / ket / ket	bra/ket/bra	bra/bra/ket	ket/bra/bra

$$\mu_{ba}\mu_{cb}\mu_{dc}\mu_{ad} \qquad \mu_{ba}^{*}\mu_{da}\mu_{cb}^{*}\mu_{cd} \qquad \mu_{ba}^{*}\mu_{cb}^{*}\mu_{da}\mu_{cd} \qquad \mu_{ba}\mu_{da}^{*}\mu_{cd}^{*}\mu_{cb}$$

$$\omega_{sig} = +\omega_1 - \omega_2 + \omega_3 \qquad -\omega_1 + \omega_2 + \omega_3 \qquad -\omega_1 + \omega_2 + \omega_3 \qquad +\omega_1 - \omega_2 + \omega_3$$

$$= \omega_{ba} + \omega_{cb} + \omega_{dc} = \omega_{da} \quad -\omega_{ba} + \omega_{da} - \omega_{cb} = \omega_{dc} \quad -\omega_{ba} - \omega_{cb} + \omega_{da} = \omega_{dc} \quad \omega_{ba} - \omega_{da} - \omega_{cd} = \omega_{bc}$$

The signal frequency comes from summing all incident resonance frequencies accounting for the sign of the excitation. The products of transition matrix elements are written in a time-ordered fashion without the projection onto the incident field polarization needed to properly account for orientational effects. The R_1 term is more properly written $\left\langle \left(\bar{\mu}_{ba} \cdot \hat{\varepsilon}_1\right)\left(\bar{\mu}_{cb} \cdot \hat{\varepsilon}_2\right)\left(\bar{\mu}_{dc} \cdot \hat{\varepsilon}_3\right)\left(\bar{\mu}_{ad} \cdot \hat{\varepsilon}_{an}\right) \right\rangle$. Note that the product of transition dipole matrix elements obtained from the sequence of interactions can always be re-written in the cyclically invariant form $\mu_{ab}\mu_{bc}\mu_{cd}\mu_{da}$ s. This is one further manifestation of closed loops formed by the sequence of interactions.

Appendix: Third-order diagrams for a vibration

The third-order nonlinear response functions for infrared vibrational spectroscopy are often applied to a weakly anharmonic vibration. For high frequency vibrations in which only the $v = 0$ state is initially populated, when the incident fields are resonant with the fundamental vibrational transition, we generally consider diagrams involving the system eigenstates $v = 0$, 1 and 2, and which include v=0-1 and v=1-2 resonances. Then, there are three distinct signal contributions:

Signal	k_{sig}	Diagrams and Transition Dipole Scaling	R/NR
S_{I}	$-k_1 + k_2 + k_3$	$\quad |\mu_{10}|^4 \qquad |\mu_{10}|^4 \qquad |\mu_{10}|^2|\mu_{21}|^2$	rephasing
S_{II}	$+k_1 - k_2 + k_3$	$\quad |\mu_{10}|^4 \qquad |\mu_{10}|^4 \qquad |\mu_{10}|^2|\mu_{21}|^2$	non-rephasing
S_{III}	$+k_1 + k_2 - k_3$	$\quad |\mu_{10}|^2|\mu_{21}|^2 \qquad |\mu_{10}|^2|\mu_{21}|^2$	non-rephasing

Note that for the S_I and S_II signals there are two types of contributions: two diagrams in which all interactions are with the v=0-1 transition (fundamental) and one diagram in which there are two interactions with v=0-1 and two with v=1-2 (the overtone). These two types of contributions have opposite signs, which can be seen by counting the number of *bra* side interactions, and have emission frequencies of ω_{10} or ω_{21}. Therefore, for harmonic oscillators, which have $\omega_{10} = \omega_{21}$ and $\sqrt{2}\mu_{10} = \mu_{21}$, we can see that the signal contributions should destructively interfere and vanish. This is a manifestation of the finding that harmonic systems display no nonlinear response. Some deviation from harmonic behavior is required to observe a signal, such as vibrational anharmonicity $\omega_{10} \neq \omega_{21}$, electrical anharmonicity $\sqrt{2}\mu_{10} \neq \mu_{21}$, or level-dependent damping $\Gamma_{10} \neq \Gamma_{21}$ or $\Gamma_{00} \neq \Gamma_{11}$.

1. D. Lee and A. C. Albrecht, "A unified view of Raman, resonance Raman, and fluorescence spectroscopy (and their analogues in two-photon absorption)." Adv. Infrared and Raman Spectr. **12**, 179 (1985).

2. To properly account for all orientational factors, the transition dipole moment must be projected onto the incident electric field polarization $\hat{\varepsilon}$ leading to the terms in the table. This leads to a nonlinear polarization that can have *x*, *y*, and *z* polarization components in the lab frame. The are obtained by projecting the matrix element prior to the final trace onto the desired analyzer axis $\hat{\varepsilon}_{an}$.

3. Prior, Y. A complete expression for the third order susceptibility $\chi^{(3)}$-perturbative and diagramatic approaches. *IEEE J. Quantum Electron.* **QE-20**, 37 (1984).
    See also, Dick, B. Response functions and susceptibilities for multiresonant nonlinear optical spectroscopy: Perturbative computer algebra solution including feeding. *Chem. Phys.* **171**, 59 (1993).

4. Bloembergen, N., Lotem, H. & Lynch, R. T. Lineshapes in coherent resonant Raman scattering. *Indian J. Pure Appl. Phys.* **16**, 151 (1978).

## 4. **Third-Order Nonlinear Spectroscopies**

Third-order nonlinear spectroscopies are the most widely used class of nonlinear methods, including the common pump-probe experiment. This section will discuss a number of these methods. The approach here is meant to be practical, with the emphasis on trying to connect the particular signals with their microscopic origin. This approach can be used for describing any experiment in terms of the wave-vector, frequency and time-ordering of the input fields, and the frequency and wavevector of the signal.

Selecting signals by wavevector

The question is how to select particular contributions to the signal. It won't be possible to uniquely select particular diagrams. However, you can use the properties of the incident and detected fields to help with selectivity. Here is a strategy for describing a particular experiment:

1) Start with the wavevector and frequency of the signal field of interest.

2) (a) Time-domain: Define a time-ordering along the incident wavevectors or

   (b) Frequency domain: Define the frequencies along the incident wavevectors.

3) Sum up diagrams for correlation functions that will scatter into the wave-vector matched direction, keeping only resonant terms (rotating wave approximation). In the frequency domain, use ladder diagrams to determine which correlation functions yield signals that pass through your filter/monochromator.

Let's start by discussing how one can distinguish a rephasing signal from a non-rephasing signal. Consider two degenerate third-order experiments ($\omega_1 = \omega_2 = \omega_3 = \omega_{sig}$) distinguished by the signal wave-vector for a particular time-ordering. We choose a box geometry, where the three incident fields (a,b,c) are crossed in the sample, incident from three corners of the box, as shown. (Colors in these figures are not meant to represent the frequency of the incident fields–which are all the

$$k_{sig} = +k_a - k_b + k_c$$
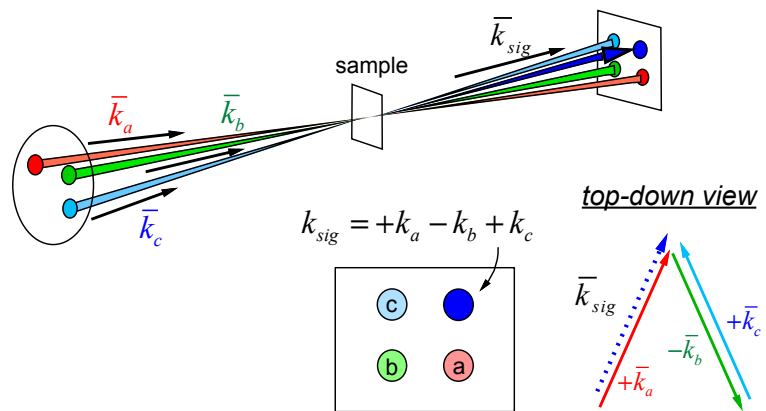
same–but rather is just there to distinguish them for the picture). Since the frequencies are the same, the length of the wavevector $|k| = 2\pi n/\lambda$ is equal for each field, only its direction varies. Vector addition of the contributing terms from the incident fields indicates that the signal $\bar{k}_{sig} = +\bar{k}_a - \bar{k}_b + \bar{k}_c$ will be radiated in the direction of the last corner of the box when observed after the sample. (Colors in the figure don't represent frequency, but serve to distinguish beams).

Comparing the wavevector matching condition for this signal with those predicted by the third-order Feynman diagrams, we see that we can select non-rephasing signals R_1 and R_4 by setting the time ordering of pulses such that $a = 1$, $b = 2$, and $c = 3$. The rephasing signals R_2 and R_3 are selected with the time-ordering $a = 2$, $b = 1$, and $c = 3$.

Alternatively, we can recognize that both signals can be observed by simultaneously detecting signals in two different directions. If we set the time ordering to be $a = 1$, $b = 2$, and $c = 3$, then the rephasing and non-rephasing signals will be radiated as shown below:
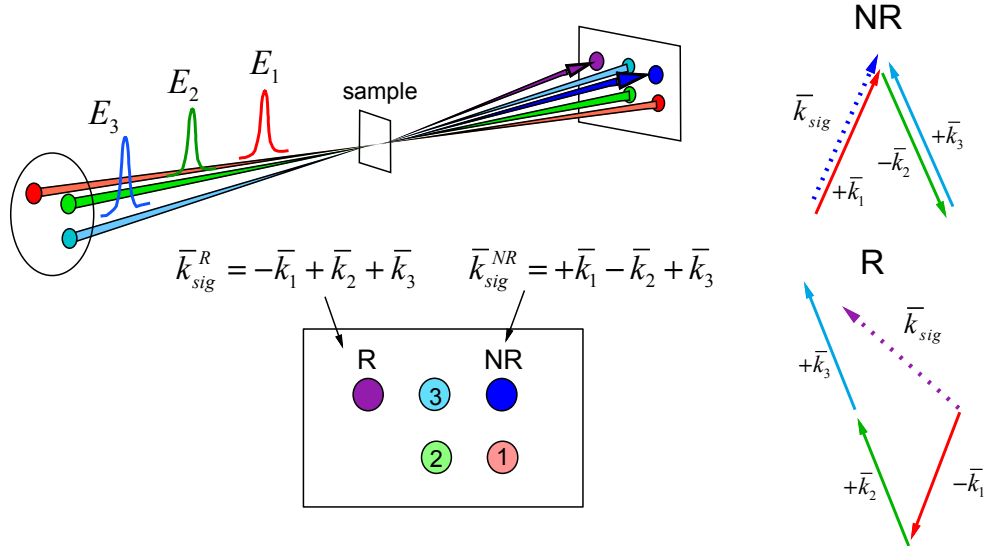
Here the wave-vector matching for the rephasing signal is imperfect. The vector sum of the incident fields $\bar{k}_{sig}$ dictates the direction of propagation of the radiated signal (momentum conservation), whereas the magnitude of the signal wavevector $\bar{k}'_{sig}$ is dictated by the radiated frequency (energy conservation). The efficiency of radiating the signal field falls of with the wave-vector mismatch $\Delta k = \bar{k}_{sig} - \bar{k}'_{sig}$, as $|\bar{E}_{sig}(t)| \propto \bar{P}(t)\,\mathrm{sinc}(\Delta kl/2)$ where l is the path length (see eq. 1.10).

Photon Echo

The photon echo experiment is most commonly used to distinguish static and dynamic line-broadening, and time-scales for energy gap fluctuations. The rephasing character of R_2 and R_3 allows you to separate homogeneous and inhomogeneous broadening. To demonstrate this let's describe a photon echo experiment for an inhomogeneous lineshape, that is a convolution of a homogeneous line shape with width Γ with a static inhomogeneous distribution of width Δ. Remember that linear spectroscopy cannot distinguish the two:
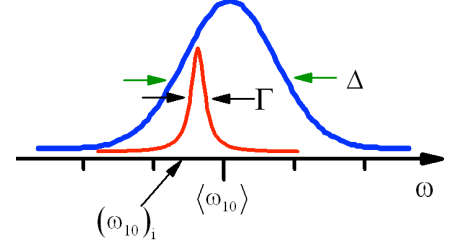
$$R(\tau) = |\mu_{ab}|^2 \, e^{-i\omega_{ab}\tau - g(\tau)} - c.c. \tag{62}$$

For an inhomogeneous distribution, we could average the homogeneous response, $g(t) = \Gamma_{ba} t$, with an inhomogeneous distribution

$$R = \int d\omega_{ab} \, G(\omega_{ab}) R(\omega_{ab}) \tag{63}$$

which we take to be Gaussian

$$G(\omega_{ba}) = \exp\left(-\frac{\left(\omega_{ba} - \langle\omega_{ba}\rangle\right)^2}{2\Delta^2} \right). \tag{64}$$

Equivalently, since a convolution in the frequency domain is a product in the time domain, we can set

$$g(t) = \Gamma_{ba} t + \tfrac{1}{2}\Delta^2 t^2. \tag{65}$$

So for the case that $\Delta > \Gamma$, the absorption spectrum is a broad Gaussian lineshape centered at the mean frequency $\langle\omega_{ba}\rangle$ which just reflects the static distribution Δ rather than the dynamics in Γ.

Now look at the experiment in which two pulses are crossed to generate a signal in the direction

$$k_{sig} = 2k_2 - k_1 \tag{66}$$

This signal is a special case of the signal $(k_3 + k_2 - k_1)$ where the second and third interactions are both derived from the same beam. Both non-rephasing diagrams contribute here, but since both second and third interactions are coincident, $\tau_2 = 0$ and $R_2 = R_3$. The nonlinear signal can be obtained by integrating the homogeneous response,

Two-pulse photon echo
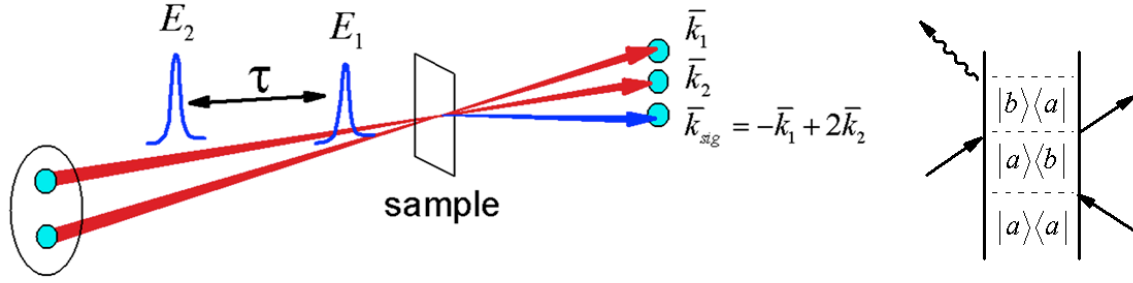
$$R^{(3)}(\omega_{ab}) = |\mu_{ab}|^4 \, p_a \, e^{-i\omega_{ab}(\tau_1-\tau_3)} e^{-\Gamma_{ab}(\tau_1+\tau_3)} \tag{67}$$

over the inhomogeneous distribution as in eq. (63). This leads to

$$R^{(3)} = |\mu_{ab}|^4 \, p_a \, e^{-i\langle\omega_{ab}\rangle(\tau_1-\tau_3)} e^{-\Gamma_{ab}(\tau_1+\tau_3)} e^{-(\tau_1-\tau_3)^2 \Delta^2/2} \tag{68}$$

For $\Delta \gg \Gamma_{ab}$, $R^{(3)}$ is sharply peaked at $\tau_1 = \tau_3$, i.e. $e^{-(\tau_1-\tau_3)^2\Delta^2/2} \approx \delta(\tau_1 - \tau_3)$. The broad distribution of frequencies rapidly dephases during τ_1, but is rephased (or refocused) during τ_3, leading to a large constructive enhancement of the polarization at $\tau_1 = \tau_3$. This rephasing enhancement is called an echo.
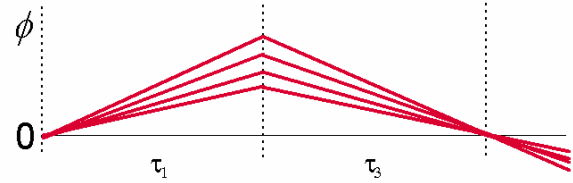
In practice, the signal is observed with a integrating intensity-level detector placed into the signal scattering direction. For a given pulse separation τ (setting $\tau_1 = \tau$), we calculated the integrated signal intensity radiated from the sample during τ_3 as

$$I_{sig}(\tau) = |E_{sig}|^2 \propto \int_{-\infty}^{\infty} d\tau_3 \left| P^{(3)}(\tau,\tau_3) \right|^2 \tag{69}$$

In the inhomogeneous limit ($\Delta \gg \Gamma_{ab}$), we find

$$I_{sig}(\tau) \propto |\mu_{ab}|^8 \, e^{-4\Gamma_{ab}\tau} . \tag{70}$$

In this case, the only source of relaxation of the polarization amplitude at $\tau_1 = \tau_3$ is Γ_{ab}. At this point inhomogeneity is removed and only the homogeneous dephasing is measured. The factor of four in the decay rate reflects the fact that damping of the initial coherence evolves over two periods $\tau_1 + \tau_3 = 2\tau$, and that an intensity level measurement doubles the decay rate of the polarization.

Transient Grating

The transient grating is a third-order technique used for characterizing numerous relaxation processes, but is uniquely suited for looking at optical excitations with well-defined spatial period. The first two pulses are set time-coincident, so you cannot distinguish which field interacts first. Therefore, the signal will have contributions both from $k_{sig} = k_1 - k_2 + k_3$ and $k_{sig} = -k_1 + k_2 + k_3$. That is the signal depends on $R_1 + R_2 + R_3 + R_4$.
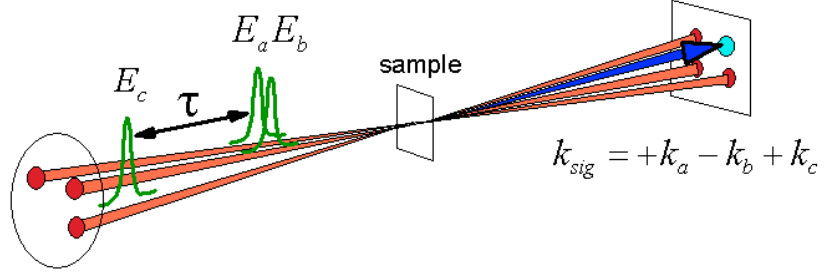
Consider the terms contributing to the polarization that arise from the first two interactions. For two time-coincident pulses of the same frequency, the first two fields have an excitation profile in the sample

$$\bar{E}_a \bar{E}_b = E_a E_b \exp\left[-i\left(\omega_a - \omega_b\right)t + i\left(\bar{k}_a - \bar{k}_b\right)\cdot\bar{r}\right] + c.c. \tag{71}$$
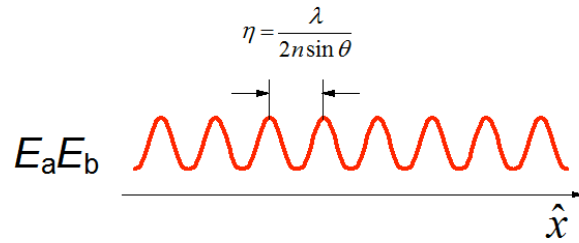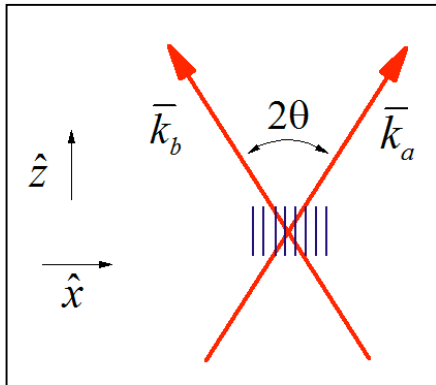
If the beams are crossed at an angle 2θ

$$\begin{aligned}
\bar{k}_a &= \left|k_a\right|\left(\hat{z}\cos\theta + \hat{x}\sin\theta\right) \\
\bar{k}_b &= \left|k_b\right|\left(\hat{z}\cos\theta - \hat{x}\sin\theta\right)
\end{aligned} \tag{72}$$

with

$$\left|k_a\right| = \left|k_b\right| = \frac{2\pi n}{\lambda}, \tag{73}$$

the excitation of the sample is a spatial varying interference pattern along the transverse direction

$$\bar{E}_a \bar{E}_b = E_a E_b \exp\left[i\bar{\beta}\cdot\bar{x}\right] + c.c. \tag{74}$$

The grating wavevector is

$$\bar{\beta} = \bar{k}_1 - \bar{k}_2$$
$$\left|\bar{\beta}\right| = \frac{4\pi n}{\lambda}\sin\theta = \frac{2\pi}{\eta}. \tag{75}$$

This spatially varying field pattern is called a grating, and has a fringe spacing

$$\eta = \frac{\lambda}{2n\sin\theta}. \tag{76}$$

Absorption images this pattern into the sample, creating a spatial pattern of excited and ground state molecules. A time-delayed probe beam can scatter off this grating, where the wavevector matching conditions are equivalent to the constructive interference of scattered waves at the Bragg angle off a diffraction grating. For $\omega_1 = \omega_2 = \omega_3 = \omega_{sig}$ this the diffraction condition is incidence of $\bar{k}_3$ at an angle θ, leading to scattering of a signal out of the sample at an angle $-\theta$. Most commonly, we measure the intensity of the scattered light, as given in eq. (69).

More generally, we should think of excitation with this pulse pair leading to a periodic spatial variation of the complex index of refraction of the medium. Absorption can create an excited state grating, whereas subsequent relaxation can lead to heating a periodic temperature profile (a thermal grating). Nonresonant scattering processes (Raleigh and Brillouin scattering) can create a spatial modulation in the real index or refraction. Thus, the transient grating signal will be sensitive to any processes which act to wash out the spatial modulation of the grating pattern:
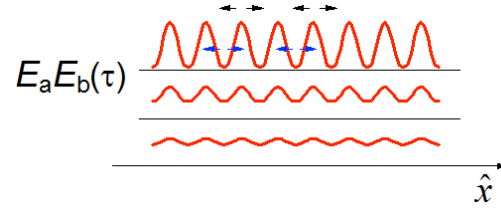
- Population relaxation leads to a decrease in the grating amplitude, observed as a decrease in diffraction efficiency.

$$I_{sig}\left(\tau\right) \propto \exp\left[-2\Gamma_{bb}\tau\right] \tag{77}$$
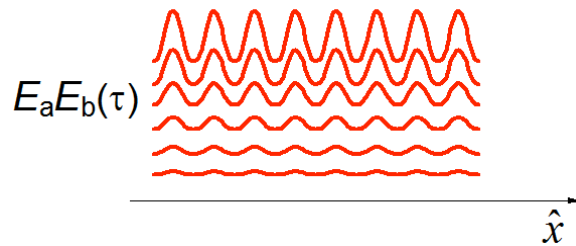
- Thermal or mass diffusion along $\hat{x}$ acts to wash out the fringe pattern. For a diffusion constant D the decay of diffraction efficiency is

$$I_{sig}(\tau) \propto \exp\left[-2\beta^2 D\tau\right] \tag{78}$$

- Rapid heating by the excitation pulses can launch counter propagating acoustic waves along $\hat{x}$, which can modulate the diffracted beam at a frequency dictated by the period for which sound propagates over the fringe spacing in the sample.
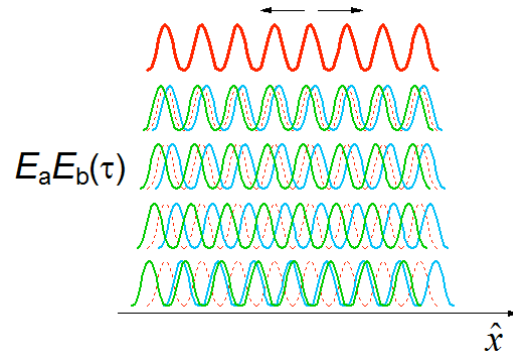
Pump-Probe

The pump-probe or transient absorption experiment is perhaps the most widely used third-order nonlinear experiment. It can be used to follow many types of time-dependent relaxation processes and chemical dynamics, and is most commonly used to follow population relaxation, chemical kinetics, or wavepacket dynamics and quantum beats.

The principle is quite simple, and the using the theoretical formalism of nonlinear spectroscopy often unnecessary to interpret the experiment. Two pulses separated by a delay τ are crossed in a sample: a pump pulse and a time-delayed probe pulse. The pump pulse E_{pu} creates a non-equilibrium state, and the time-dependent changes in the sample are characterized by the probe-pulse E_{pr} through the pump-induced intensity change on the transmitted probe, ΔI.
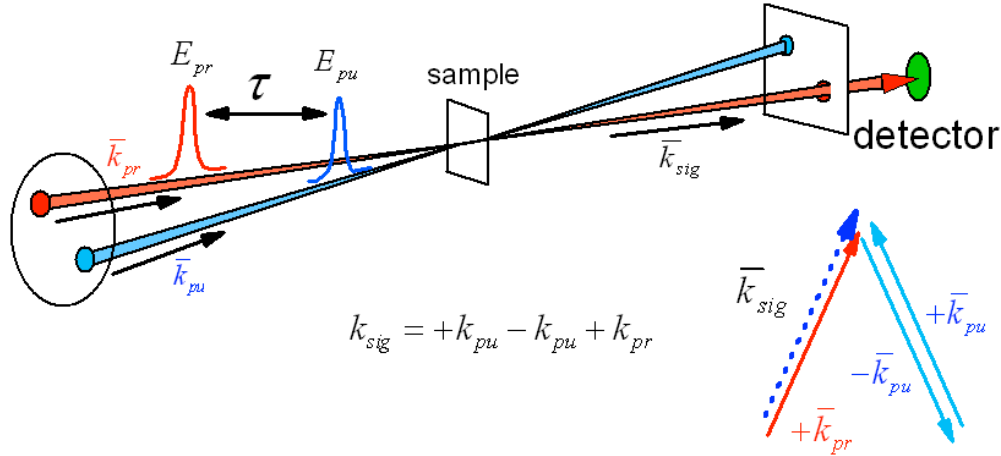
$$k_{sig} = +k_{pu} - k_{pu} + k_{pr}$$

Described as a third-order coherent nonlinear spectroscopy, the signal is radiated collinear to the transmitted probe field, so the wavevector matching condition is $\bar{k}_{sig} = +\bar{k}_{pu} - \bar{k}_{pu} + \bar{k}_{pr} = \bar{k}_{pr}$. There are two interactions with the pump field and the third interaction is with the probe. Similar to the transient grating, the time-ordering of pump-interactions cannot be distinguished, so terms that contribute to scattering along the probe are $k_{sig} = \pm k_1 \mp k_2 + k_3$ (i.e., all correlation functions R_1 to R_4). In fact, the pump-probe can be thought of as the limit of the transient grating experiment in the limit of zero grating wavevector (θ and $\beta \rightarrow 0$).

The detector observes the intensity of the transmitted probe and nonlinear signal

$$I = \frac{nc}{4\pi} \left| E'_{pr} + E_{sig} \right|^2 . \tag{79}$$

E'_{pr} is the transmitted probe field corrected for linear propagation through the sample. The measured signal is typically the differential intensity on the probe field with and without the pump field present:

$$\Delta I(\tau) = \frac{nc}{4\pi}\left\{\left|E'_{pr} + E_{sig}(\tau)\right|^2 - \left|E'_{pr}\right|^2\right\}.$$ (80)

If we work under conditions of a weak signal relative to the transmitted probe $\left|E'_{pr}\right| \gg \left|E_{sig}\right|$, then the differential intensity in eq. (80) is dominated by the cross term

$$\begin{aligned}\Delta I(\tau) &\approx \frac{nc}{4\pi}\left[E'_{pr}E^*_{sig}(\tau) + c.c.\right] \\ &= \frac{nc}{2\pi}\mathrm{Re}\left[E'_{pr}E^*_{sig}(\tau)\right]\end{aligned}$$ (81)

So the pump-probe signal is directly proportional to the nonlinear response. Since the signal field is related to the nonlinear polarization through a $\pi/2$ phase shift,

$$\bar{E}_{sig}(\tau) = i\frac{2\pi\omega_{sig}\ell}{nc}P^{(3)}(\tau).$$ (82)

the measured pump-probe signal is proportional to the imaginary part of the polarization

$$\Delta I(\tau) = 2\omega_{sig}\ell\,\mathrm{Im}\left[E'_{pr}P^{(3)}(\tau)\right],$$ (83)

which is also proportional to the correlation functions derived from the resonant diagrams we considered earlier.

Dichroic and Birefringent Response

In analogy to what we observed earlier for linear spectroscopy, the nonlinear changes in absorption of the transmitted probe field are related to the imaginary part of the susceptibility, or the imaginary part of the index of refraction. In addition to the fully resonant processes, it is also possible for the pump field to induce nonresonant changes to the polarization that modulate the real part of the index of refraction. These can be described through a variety of nonresonant interactions, such as nonresonant Raman, the optical Kerr effect, coherent Raleigh or Brillouin scattering, or the second hyperpolarizability of the sample. In this case, we can describe the time-development of the polarization and radiated signal field as

$$P^{(3)}(\tau,\tau_3) = P^{(3)}(\tau,\tau_3)e^{-i\omega_{sig}\tau_3} + \left[P^{(3)}(\tau,\tau_3)\right]^* e^{i\omega_{sig}\tau_3}$$

$$= 2\operatorname{Re}\left[P^{(3)}(\tau,\tau_3)\right]\cos(\omega_{sig}\tau_3) + 2\operatorname{Im}\left[P^{(3)}(\tau,\tau_3)\right]\sin(\omega_{sig}\tau_3) \tag{84}$$

$$\bar{E}_{sig}(\tau_3) = \frac{4\pi\omega_{sig}\ell}{nc}\left(\operatorname{Re}\left[P^{(3)}(\tau,\tau_3)\right]\sin(\omega_{sig}\tau_3) + \operatorname{Im}\left[P^{(3)}(\tau,\tau_3)\right]\cos(\omega_{sig}\tau_3)\right)$$

$$= E_{bir}(\tau,\tau_3)\sin(\omega_{sig}\tau_3) + E_{dic}(\tau,\tau_3)\cos(\omega_{sig}\tau_3) \tag{85}$$

Here the signal is expressed as a sum of two contributions, referred to as the birefringent (E_{bir}) and dichroic (E_{dic}) responses. As before the imaginary part, or dichroic response, describes the sample-induced amplitude variation in the signal field, whereas the birefringent response corresponds to the real part of the nonlinear polarization and represents the phase-shift or retardance of the signal field induced by the sample.

In this scheme, the transmitted probe is

$$\bar{E}'_{pr}(\tau_3) = E'_{pr}(\tau_3)\cos(\omega_{pr}\tau_3) , \tag{86}$$

So that the

$$\Delta I(\tau) \approx \frac{nc}{2\pi}\left[E'_{pr}(\tau)E_{dic}(\tau)\right] \tag{87}$$

Because the signal is in-quadrature with the polarization ($\pi/2$ phase shift), the absorptive or dichroic response is in-phase with the transmitted probe, whereas the birefringent part is not observed. If we allow for the phase of the probe field to be controlled, for instance through a quarter-wave plate before the sample, then we can write

$$\bar{E}'_{pr}(\tau_3,\varphi) = E'_{pr}(\tau_3)\cos(\omega_{pr}\tau_3+\varphi) , \tag{88}$$

$$I(\tau,\varphi) \approx \frac{nc}{2\pi}\left[E'_{pr}(\tau)E_{bir}(\tau)\sin(\varphi) + E'_{pr}(\tau)E_{dic}(\tau)\cos(\varphi)\right] \tag{89}$$

The birefringent and dichroic response of the molecular system can now be observed for phases of $\phi = \pi/2, 3\pi/2\ldots$ and $\phi = 0, \pi\ldots$, respectively.

Incoherent pump-probe experiments

What information does the pump-probe experiment contain? Since the time delay we control is the second time interval τ_2, the diagrams for a two level system indicate that these measure population relaxation:

$$\Delta I(\tau) \propto |\mu_{ab}|^4 \, e^{-\Gamma_{bb}\tau} \tag{90}$$

In fact measuring population changes and relaxation are the most common use of this experiment. When dephasing is very rapid, the pump-probe can be interpreted as an incoherent experiment, and the differential intensity (or absorption) change is proportional to the change of population of the states observed by the probe field. The pump-induced population changes in the probe states can be described by rate equations that describe the population relaxation, redistribution, or chemical kinetics.

For the case where the pump and probe frequencies are the same, the signal decays as a results of population relaxation of the initially excited state. The two-level system diagrams indicate that the evolution in τ_2 is differentiated by evolution in the ground or excited state. These diagrams reflect the equal signal contributions from the ground state bleach (loss of ground state population) and stimulated emission from the excited state. For direct relaxation from excited to ground state the loss of population in the excited state Γ_{bb} is the same as the refilling of the hole in the ground state Γ_{aa}, so that $\Gamma_{aa} = \Gamma_{bb}$. If population relaxation from the excited state is through an intermediate, then the pump-probe decay will reflect equal contributions from both processes, which can be described by coupled first-order rate equations.

When the resonance frequencies of the pump and probe fields are different, then the incoherent pump-probe signal is related to the joint probability of exciting the system at ω_{pu} and detecting at ω_{pr} after waiting a time τ, $P(\omega_{pr}, \tau; \omega_{pu})$.

### *Coherent pump-probe experiments*

Ultrafast pump-probe measurements on the time-scale of vibrational dephasing operate in a coherent regime where wavepackets prepared by the pump-pulse modulate the probe intensity. This provides a mechanism for studying the dynamics of excited electronic states with coupled vibrations and photoinitiated chemical reaction dynamics. If we consider the case of pump-probe
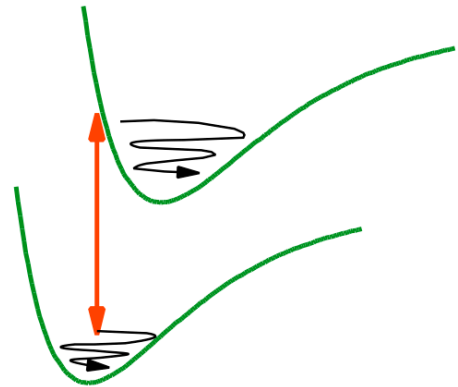
experiments on electronic states where $\omega_{pu} = \omega_{pr}$, our description of the pump-probe from Feynmann diagrams indicates that the pump-pulse creates excitations both on the excited state and ground state. Both wavepackets will contribute to the signal.

There are two equivalent ways of describing the experiment, which mirror our earlier description of electronic spectroscopy for an electronic transition coupled to nuclear motion. The first is to describe the spectroscopy in terms of the eigenstates of H_0, $|e,n\rangle$. The second draws on the energy gap Hamiltonian to describe the spectroscopy as two electronic levels H_S that interact with the vibrational degrees of freedom H_B, and the wavepacket dynamics are captured by H_{SB}.

For the eigenstate description, a two level system is inadequate to capture the wavepacket dynamics. Instead, describe the spectroscopy in terms of the four-level system diagrams given earlier. In addition to the population relaxation terms, we see that the R_2 and R_4 terms describe the evolution of coherences in the excited electronic state, whereas the R_1 and R_3 terms describe the ground state wave packet. For an underdamped wavepacket these coherences are observed as quantum beats on the pump-probe signal.
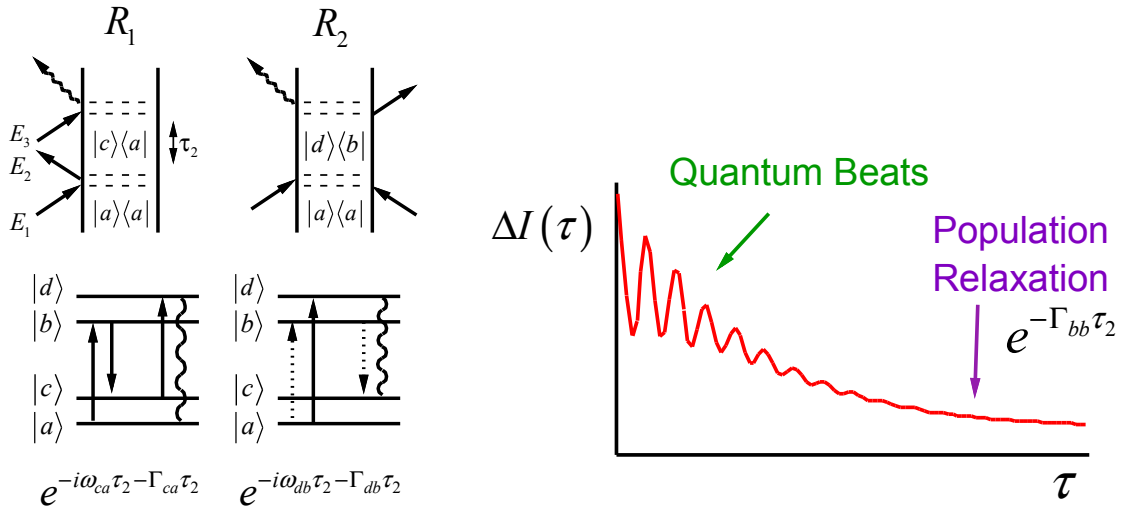
CARS (Coherent Anti-Stokes Raman Scattering)

Used to drive ground state vibrations with optical pulses or cw fields.

- Two fields, with a frequency difference equal to a vibrational transition energy, are used to excite the vibration.

- The first field is the "pump" and the second is the "Stokes" field.

- A second interaction with the pump frequency lead to a signal that radiates at the anti-Stokes frequency: $\omega_{sig} = 2\omega_P - \omega_S$ and the signal is observed background-free next to the transmitted pump field: $\bar{k}_{sig} = 2\bar{k}_P - \bar{k}_S$.
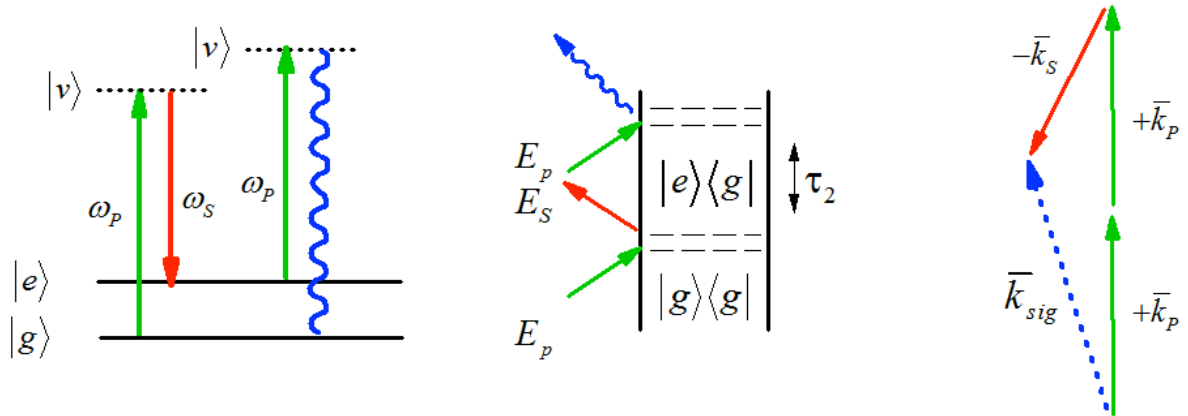
The experiment is described by R$_1$ to R$_4$, and the polarization is

$$R^{(3)} = \bar{\mu}_{ev'}\bar{\mu}_{v'g}\, e^{-i\omega_{eg}\tau - \Gamma_{eg}\tau}\, \bar{\mu}_{gv}\bar{\mu}_{ve} + c.c.$$
$$= \bar{\alpha}_{eg} e^{-i\omega_{eg}\tau - \Gamma_{eg}\tau}\, \bar{\alpha}_{ge} + c.c.$$

The CARS experiment is similar to a linear experiment in which the lineshape is determined by the Fourier transform of $C(\tau) = \langle \bar{\alpha}(\tau)\bar{\alpha}(0) \rangle$.

The same processes contribute to Optical Kerr Effect Experiments and Impulsive Stimulated Raman Scattering.

5. <u>Characterizing Fluctuations</u>

<u>Eigenstate vs. system/bath perspectives</u>

From our earlier work on electronic spectroscopy, we found that there are two equivalent ways of describing spectroscopic problems, which can be classified as the eigenstate and system/bath perspectives. Let's summarize these before turning back to nonlinear spectroscopy, using electronic spectroscopy as the example:

1) <u>Eigenstate</u>: The interaction of light and matter is treated with the interaction picture Hamiltonian $H = H_0 + V(t)$. H_0 is the full material Hamiltonian, expressed as a function of nuclear and electronic coordinates, and is characterized by eigenstates which are the solution to $H_0|n\rangle = E_n|n\rangle$. In the electronic case $|n\rangle = |e, n_1, n_2 ...\rangle$ represent labels for a particular vibronic state. The dipole operator in $V(t)$ couples these states. Given that we have such detailed knowledge of the matter, we can obtain an absorption spectrum in two ways. In the time domain, we know

$$C_{\mu\mu}(t) = \sum_n p_n \langle n|\mu(t)\mu(0)|n\rangle = \sum_{n,m} p_n |\mu_{nm}|^2 e^{-i\omega_{mn}t} \qquad (91)$$

The absorption lineshape is then related to the Fourier transform of $C(t)$,

$$\sigma(\omega) = \sum_{n,m} p_n |\mu_{nm}|^2 \frac{1}{\omega - \omega_{nm} - i\Gamma_{nm}} \qquad (92)$$

where the phenomenological damping constant Γ_{nm} was first added into eq. (91). This approach works well if you have an intimate knowledge of the Hamiltonian if your spectrum is highly structured and if irreversible relaxation processes are of minor importance.

2) <u>System/Bath</u>: In condensed phases, irreversible dynamics and featureless lineshapes suggest a different approach. In the system/bath or energy gap representation, we separate our Hamiltonian into two parts: the system H_S contains a few degrees of freedom Q which we treat in detail, and the remaining degrees of freedom (q) are in the bath H_B. Ideally, the interaction between the two sets $H_{SB}(qQ)$ is weak.

$$H_0 = H_S + H_B + H_{SB}. \qquad (93)$$

Spectroscopically we usually think of the dipole operator as acting on the system state, i.e. the dipole operator is a function of Q. If we then know the eigenstates of H_S, $H_S |n\rangle = E_n |n\rangle$ where $|n\rangle = |g\rangle$ or $|e\rangle$ for the electronic case, the dipole correlation function is

$$C_{\mu\mu}(t) = |\mu_{eg}|^2 e^{-i\langle\omega_{eg}\rangle t} \left\langle \exp\left[-i\int_0^t H_{SB}(t')dt'\right]\right\rangle \tag{94}$$

The influence of the dark states in H_B is to modulate or change the spectroscopic energy gap ω_{eg} in a form dictated by the time-dependent system-bath interaction. The system-bath approach is a natural way of treating condensed phase problems where you can't treat all of the nuclear motions (liquid/lattice) explicitly. Also, you can imagine hybrid approaches if there are several system states that you wish to investigate spectroscopically.

Energy Gap Fluctuations

How do transition energy gap fluctuations enter into the nonlinear response? As we did in the case of linear experiments, we will make use of the second cumulants approximation to relate dipole correlation functions to the energy gap correlation function $C_{eg}(\tau)$. Remembering that for the case of a system-bath interaction that that linearly couples the system and bath nuclear coordinates, the cumulant expansion allows the linear spectroscopy to be expressed in terms of the lineshape function $g(t)$

$$C_{\mu\mu}(t) = |\mu_{eg}|^2 e^{-i\omega_{eg}t} e^{-g(t)} \tag{95}$$

$$g(t) = \int_0^t dt'' \int_0^{t''} dt' \underbrace{\frac{1}{\hbar^2}\left\langle \delta H_{eg}(t')\delta H_{eg}(0)\right\rangle}_{C_{eg}(t')} \tag{96}$$

$$C_{eg}(\tau) = \left\langle \delta\omega_{eg}(\tau)\delta\omega_{eg}(0)\right\rangle \tag{97}$$

$g(t)$ is a complex function for which the imaginary components describe nuclear motion modulating or shifting the energy gap, whereas the real part describes the fluctuations and

damping that lead to line broadening. When $C_{eg}(\tau)$ takes on an undamped oscillatory form $C_{eg}(\tau) = De^{i\omega_0\tau}$, as we might expect for coupling of the electronic transition to a nuclear mode with frequency ω_0, we recover the expressions that we originally derived for the electronic absorption lineshape in which D is the coupling strength and related to the Frank-Condon factor.

Here we are interested in discerning line-broadening mechanisms, and the time scale of random fluctuations that influence the transition energy gap. Summarizing our earlier results, we can express the lineshape functions for energy gap fluctuations in the homogeneous and imhomogeneous limit as

1) Homogeneous. The bath fluctuations are infinitely fast, and only characterized by a magnitude:

$$C_{eg}(\tau) = \Gamma\delta(\tau).$$ (98)

In this limit, we obtain the phenomenological damping result

$$g(t) = \Gamma t$$ (99)

Which leads to homogeneous Lorentzian lineshapes with width Γ.

2) Inhomogeneous. The bath fluctuations are infinitely slow, and again characterized by a magnitude, but there is no decay of the correlations

$$C_{eg}(\tau) = \Delta^2.$$ (100)

This limit recovers the Gaussian static limit, and the Gaussian inhomogeneous lineshape where Δ is the distribution of frequencies.

$$g(t) = \tfrac{1}{2}\Delta^2 t^2.$$ (101)

3) The intermediate regime is when the energy gap fluctuates on the same time scale as the experiment. The simplest description is the stochastic model which describes the loss of correlation with a time scale τ_c

$$C_{eg}(\tau) = \Delta^2 \exp(-t/\tau_c)$$ (102)

which leads to

$$g(t) = \Delta^2 \tau_c^2 \left[\exp(-t/\tau_c) + t/\tau_c - 1\right]$$ (103)

For an arbitrary form of the dynamics of the bath, we can construct $g(t)$ as a sum over independent modes $g(t) = \sum_i g_i(t)$. Or for a continuous distribution for modes, we can describe the bath in terms of the spectral density $\rho(\omega)$ that describes the coupled nuclear motions

$$\rho(\omega) = \frac{1}{2\pi\omega^2} \text{Im}\left[\tilde{C}_{eg}(\omega)\right] \tag{104}$$

$$\begin{aligned} g(t) &= \int_{-\infty}^{+\infty} d\omega \frac{1}{2\pi\omega^2} \tilde{C}_{eg}(\omega)\left[\exp(-i\omega t) + i\omega t - 1\right] \\ &= \int_{-\infty}^{+\infty} d\omega\, \rho(\omega)\left(\coth\left(\frac{\beta\hbar\omega}{2}\right)(1-\cos\omega t) + i(\sin\omega t - \omega t)\right) \end{aligned} \tag{105}$$

To construct an arbitrary form of the bath, the phenomenological Brownian oscillator model allows us to construct a bath of i damped oscillators,

$$\begin{aligned} C''_{eg}(\omega) &= \sum_i \xi_i C''_i(\omega) \\ C''_i(\omega) &= \frac{\hbar}{m_i} \frac{\omega\Gamma_i}{\left(\omega_i^2 - \omega^2\right)^2 + 4\omega^2\Gamma_i^2} \end{aligned} \tag{106}$$

Here ξ_i is the coupling coefficient for oscillator i.

Nonlinear Response with the Energy Gap Hamiltonian

In a manner that parallels our description of the linear response from a system coupled to a bath, the nonlinear response can also be partitioned into a system, bath and energy gap Hamiltonian, leading to similar averages over the fluctuations of the energy gap. In the general case, the four correlations functions contributing to the third order response that emerge from eq. (37) are

$$\begin{aligned} R_1 &= \sum_{abcd} p_a \left\langle \mu_{ab}(\tau_3 + \tau_2 + \tau_1)\mu_{bc}(\tau_2 + \tau_1)\mu_{cd}(\tau_1)\mu_{da}(0) F^{(1)}_{abcd} \right\rangle \\ R_2 &= \sum_{abcd} p_a \left\langle \mu_{ab}(\tau_1)\mu_{bc}(\tau_2 + \tau_1)\mu_{cd}(\tau_3 + \tau_2 + \tau_1)\mu_{da}(0) F^{(2)}_{abcd} \right\rangle \\ R_3 &= \sum_{abcd} p_a \left\langle \mu_{da}(0)\mu_{ab}(\tau_2 + \tau_1)\mu_{bc}(\tau_3 + \tau_2 + \tau_1)\mu_{cd}(\tau_1) F^{(3)}_{abcd} \right\rangle \\ R_4 &= \sum_{abcd} p_a \left\langle \mu_{da}(\tau_1)\mu_{ab}(t_1)\mu_{bc}(\tau_3 + \tau_2 + \tau_1)\mu_{cd}(\tau_2 + \tau_1) F^{(4)}_{abcd} \right\rangle \end{aligned} \tag{107}$$

Here $a,b,c,$ and d are indices for system eigenstates, and the dephasing functions are

$$F_{abcd}^{(1)} = \exp\left[-i\int_{\tau_2+\tau_1}^{\tau_3+\tau_2+\tau_1}\omega_{ba}(\tau)d\tau - i\int_{\tau_1}^{\tau_2+\tau_1}\omega_{ca}(\tau)d\tau - i\int_0^{\tau_1}\omega_{da}(\tau)d\tau\right]$$

$$F_{abcd}^{(2)} = \exp\left[-i\int_{\tau_2+\tau_1}^{\tau_3+\tau_2+\tau_1}\omega_{dc}(\tau)d\tau - i\int_{\tau_1}^{\tau_2+\tau_1}\omega_{db}(\tau)d\tau - i\int_0^{\tau_1}\omega_{da}(\tau)d\tau\right]$$

$$F_{abcd}^{(3)} = \exp\left[-i\int_{\tau_2+\tau_1}^{\tau_3+\tau_2+\tau_1}\omega_{bc}(\tau)d\tau + i\int_{\tau_1}^{\tau_2+\tau_1}\omega_{ca}(\tau)d\tau + i\int_0^{\tau_1}\omega_{da}(\tau)d\tau\right]$$

$$F_{abcd}^{(4)} = \exp\left[-i\int_{\tau_2+\tau_1}^{\tau_3+\tau_2+\tau_1}\omega_{bc}(\tau)d\tau + i\int_{\tau_1}^{\tau_2+\tau_1}\omega_{db}(\tau)d\tau + i\int_0^{\tau_1}\omega_{da}(\tau)d\tau\right]$$

(108)

As before $\omega_{ab} = H_{ab}/\hbar$. These expressions describe the correlated dynamics of the dipole operator acting between multiple resonant transitions, in which the amplitude, frequency, and orientation of the dipole operator may vary with time.

As a further simplification, let's consider the specific form of the nonlinear response for a fluctuating two-level system. If we allow only for two states e and g, and apply the Condon approximation, eq. (108) gives

$$R_1\left(\tau_1,\tau_2,\tau_3\right) = p_g\left|\mu_{eg}\right|^4 e^{i\omega_{eg}(\tau_1+\tau_3)}\left\langle\exp\left(-i\int_0^{\tau_1}d\tau\,\omega_{eg}(\tau) - i\int_{\tau_1+\tau_2}^{\tau_1+\tau_2+\tau_3}d\tau\,\omega_{eg}(\tau)\right)\right\rangle$$ (109)

$$R_2\left(\tau_1,\tau_2,\tau_3\right) = p_g\left|\mu_{eg}\right|^4 e^{-i\omega_{eg}(\tau_1-\tau_3)}\left\langle\exp\left(i\int_0^{\tau_1}d\tau\,\omega_{eg}(\tau) - i\int_{\tau_1+\tau_2}^{\tau_1+\tau_2+\tau_3}d\tau\,\omega_{eg}(\tau)\right)\right\rangle$$ (110)

These are the rephasing (R_2) and non-rephasing (R_1) functions, written for a two-level system. These expressions only account for the correlation of fluctuating frequencies while the system evolves during the coherence periods τ_1 and τ_3. Since they neglect any difference in relaxation on the ground or excited state during the population period τ_2, $R_2 = R_3$ and $R_1 = R_4$. They also ignore reorientational relaxation of the dipole.

In the case that the fluctuations of those two states follow Gaussian statistics, we can also apply the cumulant expansion to the third order response function. In this case, for a two-level system, the four correlation functions are expressed in terms of the lineshape function as:

$$R_1 = e^{-i\omega_{eg}\tau_1 - i\omega_{eg}\tau_3} \left(\frac{i}{\hbar}\right)^3 p_g \left|\mu_{eg}\right|^4$$

$$\times \exp\left[-g^*(\tau_3) - g(\tau_1) - g^*(\tau_2) + g^*(\tau_2 + \tau_3) + g(\tau_1 + \tau_2) - g(\tau_1 + \tau_2 + \tau_3)\right] \qquad (111)$$

$$R_2 = \left(\frac{i}{\hbar}\right)^3 p_g \left|\mu_{eg}\right|^4 e^{i\omega_{eg}\tau_1 - i\omega_{eg}\tau_3}$$

$$\times \exp\left[-g^*(\tau_3) - g^*(\tau_1) + g(\tau_2) - g(\tau_2 + \tau_3) - g^*(\tau_1 + \tau_2) + g^*(\tau_1 + \tau_2 + \tau_3)\right] \qquad (112)$$

$$R_3 = \left(\frac{i}{\hbar}\right)^3 p_g \left|\mu_{eg}\right|^4 e^{i\omega_{eg}\tau_1 - i\omega_{eg}\tau_3}$$

$$\times \exp\left[-g(\tau_3) - g^*(\tau_1) + g^*(\tau_2) - g^*(\tau_2 + \tau_3) - g^*(\tau_1 + \tau_2) + g^*(\tau_1 + \tau_2 + \tau_3)\right] \qquad (113)$$

$$R_4 = \left(\frac{i}{\hbar}\right)^3 p_g \left|\mu_{eg}\right|^4 e^{-i\omega_{eg}\tau_1 - i\omega_{eg}\tau_3}$$

$$\times \exp\left[-g(\tau_3) - g(\tau_1) - g(\tau_2) + g(\tau_2 + \tau_3) + g(\tau_1 + \tau_2) - g(\tau_1 + \tau_2 + \tau_3)\right] \qquad (114)$$

These expressions provide the most direct way of accounting for fluctuations or periodic modulation of the spectroscopic energy gap in nonlinear spectroscopies.

Example: For the two-pulse photon echo experiment on a system with inhomogeneous broadening:

- Set $g(t) = \Gamma_{eg} t + \frac{1}{2}\Delta^2 t^2$. For this simple model $g(t)$ is real.

- Set $\tau_2 = 0$, giving

$$R_2 = R_3 = \left(\frac{i}{\hbar}\right)^3 p_g \left|\mu_{eg}\right|^4 e^{i\omega_{eg}\tau_1 - i\omega_{eg}\tau_3} \exp\left[-2g(\tau_3) - 2g(\tau_1) + g(\tau_1 + \tau_3)\right].$$

- Substituting $g(t)$ into this expression gives the same result as before.

$$R^{(3)} \propto e^{-i\omega_{eg}(\tau_1 - \tau_3)} e^{-\Gamma_{eg}(\tau_1 + \tau_3)} e^{-(\tau_1 - \tau_3)^2 \Delta^2/2} \qquad (115)$$

Similar expressions can also be derived for an arbitrary number of eigenstates of the system Hamiltonian.[8] In that case, eqs. (107) become

$$R_1 = \sum_{abcd} p_a \mu_{ab}\mu_{bc}\mu_{cd}\mu_{da} \exp\left[-i\langle\omega_{ba}\rangle\tau_3 - i\langle\omega_{ca}\rangle\tau_2 - i\langle\omega_{da}\rangle\tau_1\right] F^{(1)}_{abcd}\left(\tau_3,\tau_2,\tau_1\right)$$

$$R_2 = \sum_{abcd} p_a \mu_{ab}\mu_{bc}\mu_{cd}\mu_{da} \exp\left[-i\langle\omega_{dc}\rangle\tau_3 - i\langle\omega_{db}\rangle\tau_2 - i\langle\omega_{da}\rangle\tau_1\right] F^{(2)}_{abcd}\left(\tau_3,\tau_2,\tau_1\right)$$

$$R_3 = \sum_{abcd} p_a \mu_{ab}\mu_{bc}\mu_{cd}\mu_{da} \exp\left[-i\langle\omega_{bc}\rangle\tau_3 + i\langle\omega_{ca}\rangle\tau_2 + i\langle\omega_{da}\rangle\tau_1\right] F^{(3)}_{abcd}\left(\tau_3,\tau_2,\tau_1\right)$$

$$R_4 = \sum_{abcd} p_a \mu_{ab}\mu_{bc}\mu_{cd}\mu_{da} \exp\left[-i\langle\omega_{bc}\rangle\tau_3 + i\langle\omega_{db}\rangle\tau_2 + i\langle\omega_{da}\rangle\tau_1\right] F^{(4)}_{abcd}\left(\tau_3,\tau_2,\tau_1\right)$$

(116)

The dephasing functions are written in terms of lineshape functions with a somewhat different form:

$$-\ln\left[F^{(1)}_{abcd}\left(\tau_3,\tau_2,\tau_1\right)\right] = h_{bb}\left(\tau_3\right) + h_{cc}\left(\tau_2\right) + h_{dd}\left(\tau_1\right) + h^+_{bc}\left(\tau_3,\tau_2\right)$$
$$+ h^+_{cd}\left(\tau_3,\tau_2\right) + f^+_{bd}\left(\tau_3,\tau_1;\tau_2\right)$$

$$-\ln\left[F^{(2)}_{abcd}\left(\tau_3,\tau_2,\tau_1\right)\right] = \left[h_{cc}\left(\tau_3\right)\right]^* + \left[h_{bb}\left(\tau_2\right)\right]^* + h_{dd}\left(\tau_1+\tau_2+\tau_3\right) + \left[h^+_{bc}\left(\tau_3,\tau_2\right)\right]^*$$
$$+ h^-_{cd}\left(\tau_1+\tau_2+\tau_3,\tau_3\right) + \left[f^-_{bd}\left(\tau_2,\tau_1+\tau_2+\tau_3;\tau_3\right)\right]^*$$

$$-\ln\left[F^{(3)}_{abcd}\left(\tau_3,\tau_2,\tau_1\right)\right]^* = \left[h_{bb}\left(\tau_3\right)\right]^* + h_{cc}\left(\tau_2+\tau_3\right) + h_{dd}\left(\tau_1\right) + h^+_{cd}\left(\tau_2+\tau_3,\tau_1\right)$$
$$- f^-_{bc}\left(\tau_3,\tau_2+\tau_3;\tau_2\right) - f^+_{bd}\left(\tau_3,\tau_1;\tau_2\right)$$

$$-\ln\left[F^{(4)}_{abcd}\left(\tau_3,\tau_2,\tau_1\right)\right]^* = h_{cc}\left(\tau_3\right) + h_{dd}\left(\tau_1+\tau_2\right) + \left[h_{bb}\left(\tau_2+\tau_3\right)\right]^* - h^-_{bc}\left(\tau_3,\tau_2+\tau_3\right)$$
$$+ h^+_{cd}\left(\tau_1+\tau_2,\tau_3\right) - f^-_{bd}\left(\tau_1+\tau_2,\tau_2+\tau_3;\tau_3\right)$$

(117)

where:

$$h_{nm}\left(\tau\right) = \int_0^\tau d\tau_2' \int_0^{\tau_2} d\tau_1' C_{nm}\left(\tau_2' - \tau_1'\right)$$

$$h^\pm_{nm}\left(\tau_2,\tau_1\right) = \int_0^{\tau_2} d\tau_2' \int_0^{\tau_1} d\tau_1' C_{nm}\left(\tau_2' \pm \tau_1'\right)$$

$$f^\pm_{nm}\left(\tau_2,\tau_1;\tau_3\right) = \int_0^{\tau_2} d\tau_2' \int_0^{\tau_1} d\tau_1' C_{nm}\left(\tau_2' \pm \tau_1' + \tau_3\right).$$

(118)

---

[8] J. Sung and R. J. Silbey, "Four-wave mixing spectroscopy for a multi-level system," J. Chem. Phys. 115, 9266 (2001).

How can you characterize fluctuations and spectral diffusion?

The rephasing ability of the photon echo experiment provides a way of characterizing memory of the energy gap transition frequency initially excited by the first pulse. For a static inhomogeneous lineshape, perfect memory of transition frequencies is retained through the experiment, whereas homogeneous broadening implies extremely rapid dephasing. So, let's first examine the polarization for a two-pulse photon echo experiment on a system with homogeneous and inhomogeneous broadening by varying Δ / Γ_{eg}. Plotting the polarization as proportional to the response in eq. (115):
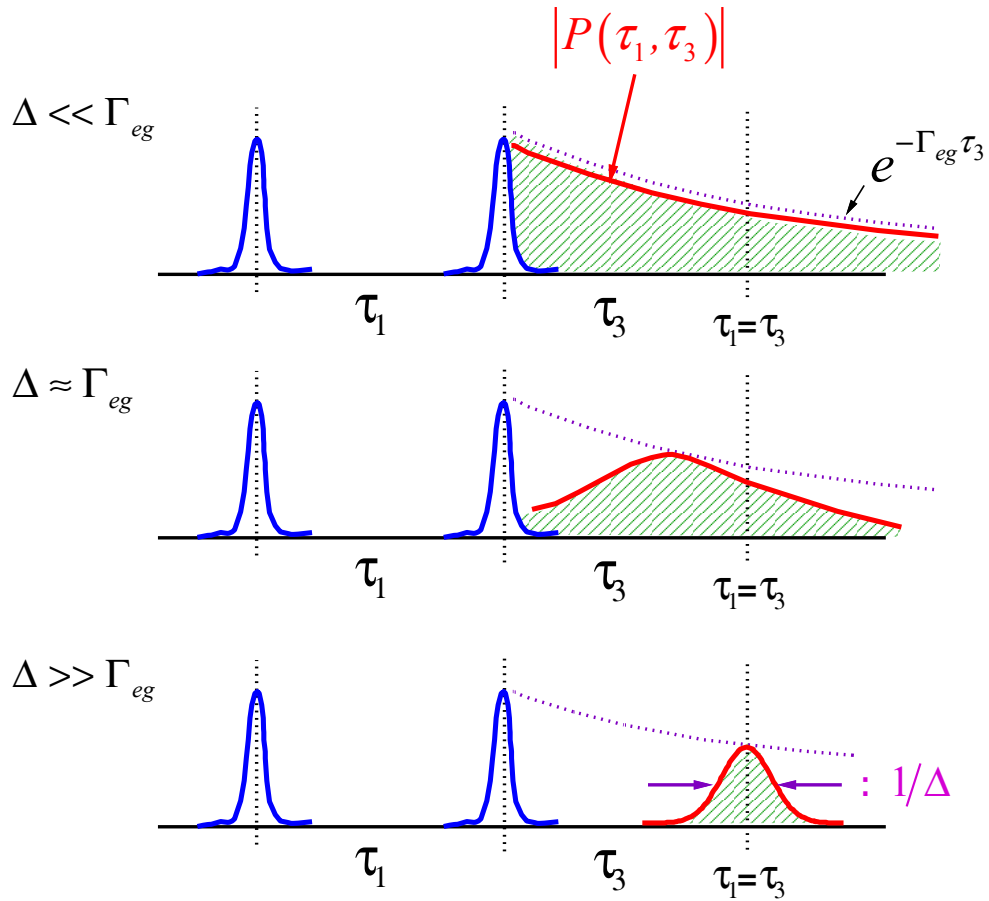
We see that following the third pulse, the polarization (red line) is damped during τ_3 through homogeneous dephasing at a rate Γ_{eg}, regardless of Δ. However in the inhomogeneous case $\Delta \gg \Gamma_{eg}$, any inhomogeneity is rephased at $\tau_1 = \tau_3$. The shape of this echo is a Gaussian with width $\sim 1/\Delta$. The shape of the echo polarization is a competition between the homogeneous damping and the inhomogeneous rephasing.

Normally, one detects the integrated intensity of the radiated echo field. Setting the pulse delay $\tau_1 = \tau$,

$$S(\tau) \propto \int_0^\infty d\tau_3 \left| P^{(3)}(\tau, \tau_3) \right|^2 \tag{119}$$

$$S(\tau) = \exp\left(-4\Gamma_{eg}\tau - \frac{\Gamma_{eg}^2}{\Delta^2} \right) \cdot \mathrm{erfc}\left(-\Delta\tau + \frac{\Gamma_{eg}}{\Delta} \right), \tag{120}$$

where $erfc(x) = 1 - erf(x)$ is the complementary error function. For the homogeneous and inhomogeneous limits of this expression we find

$$\Delta \ll \Gamma_{eg} \quad \Rightarrow \quad S(\tau) \propto e^{-2\Gamma_{eg}\tau} \tag{121}$$

$$\Delta \gg \Gamma_{eg} \quad \Rightarrow \quad S(\tau) \propto e^{-4\Gamma_{eg}\tau} \tag{122}$$

In either limit, the inhomogeneity is removed from the measured decay.

In the intermediate case, we observe that the leading term in eq. (120) decays whereas the second term rises with time. This reflects the competition between homogeneous damping and the inhomogeneous rephasing. As a result, for the intermediate case $(\Delta \approx \Gamma_{ab})$ we find that the integrated signal $S(\tau)$ has a maximum signal for $\tau > 0$.
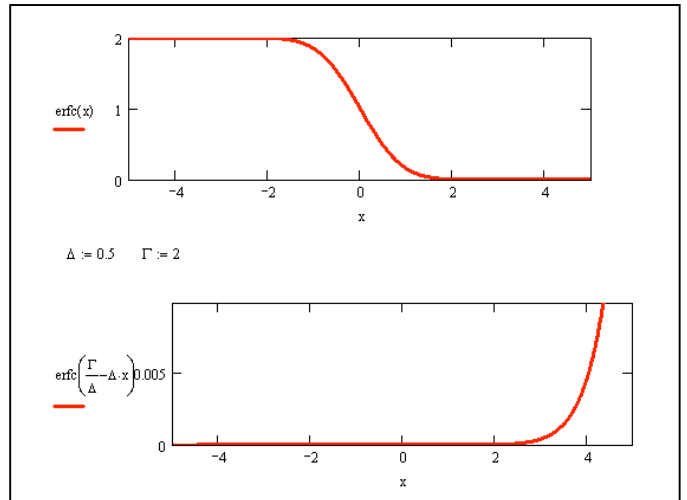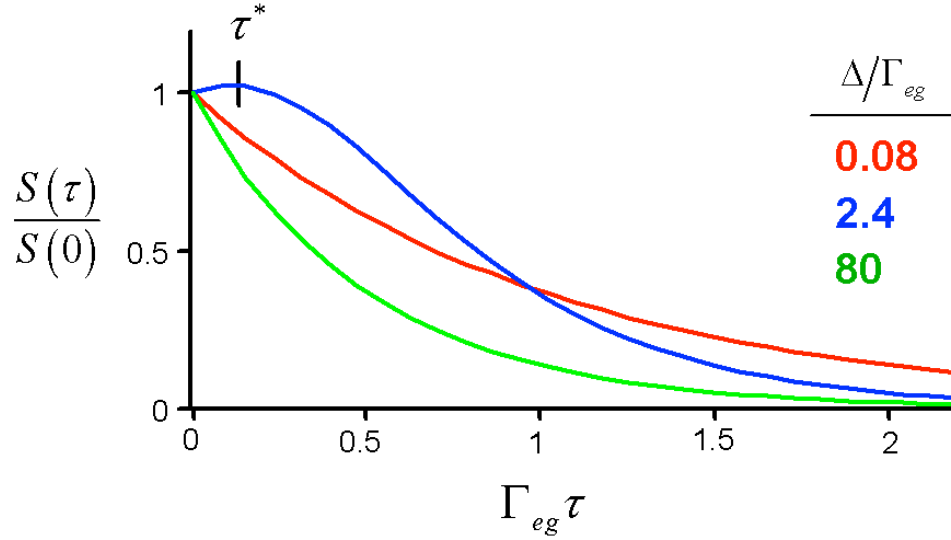
The delay of maximum signal, τ^*, is known as the peak shift. The observation of a peak shift is an indication that there is imperfect ability to rephrase. Homogenous dephasing, i.e. fluctuations fast on the time scale of τ, are acting to scramble memory of the phase of the coherence initially created by the first pulse.

In the same way, spectral diffusion (processes which randomly modulate the energy gap on time scales equal or longer than τ) randomizes phase. It destroys the ability for an echo to form by rephasing. To characterize these processes through an energy gap correlation function, we can perform a three-pulse photon echo experiment. The three pulse experiment introduces a waiting time τ_2 between the two coherence periods, which acts to define a variable shutter speed for the experiment. The system evolves as a population during this period, and therefore there is nominally no phase acquired. We can illustrate this through a lens analogy:

Lens Analogy: For an inhomogeneous distribution of oscillators with different frequencies, we define the phase acquired during a time period through $e^{i\phi} = e^{i(\delta\omega_i t)}$.

**Two-Pulse Photon Echo:**
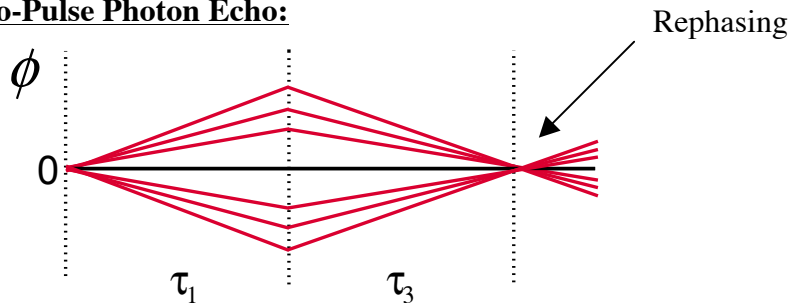
Three-Pulse Photon Echo:
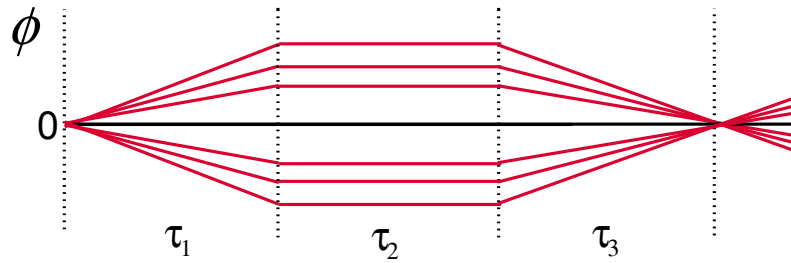
Since we are in a population state during τ_2, there is no evolution of phase. Now to this picture we can add spectral diffusion as a slower random modulation of the phase acquired during all time periods. If the system can spectrally diffuse during τ_2, this degrades the ability of the system to rephase and echo formation is diminished.

Three-Pulse Photon Echo with Spectral Diffusion:
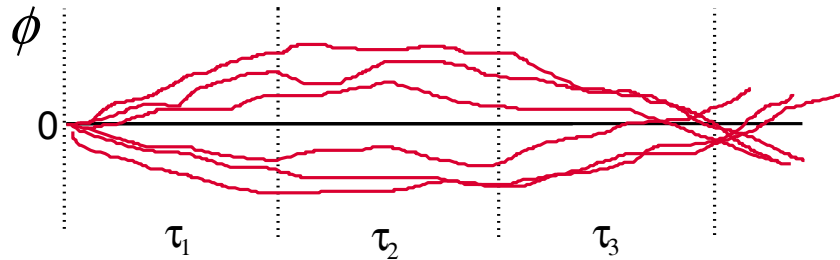
Since spectral diffusion destroys the rephasing, the system appears more and more "homogeneous" as τ_2 is incremented. Experimentally, one observes how the peak shift of the integrated echo changes with the waiting time τ_2. It will be observed to shift toward $\tau^* = 0$ as a function of τ_2.
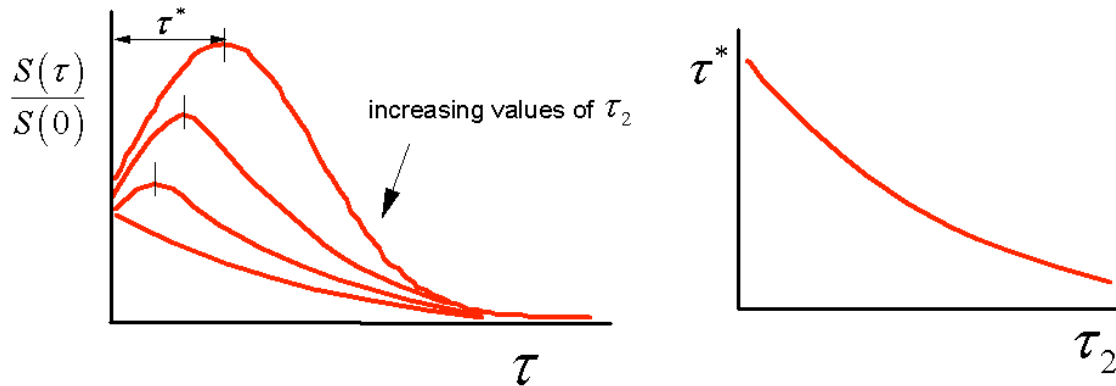
In fact, one can show that the peak shift with τ_2 decays with a form given by the the correlation function for system-bath interactions:

$$\tau^*(\tau_2) \propto C_{eg}(\tau) \tag{123}$$

Using the lineshape function for the stochastic model $g(t) = \Delta^2 \tau_c^2 \left[\exp(-t/\tau_c) + t/\tau_c - 1\right]$, you can see that for times $\tau_2 > \tau_c$,

$$\tau^*(\tau_2) \propto \exp(-\tau_2/\tau_c) \Rightarrow \left\langle \delta\omega_{eg}(\tau)\delta\omega_{eg}(0)\right\rangle \tag{124}$$

Thus echo peak shift measurements are a general method to determine the form to $C_{eg}(\tau)$ or $C_{eg}''(\omega)$ or $\rho(\omega)$. The measurement time scale is limited only by the population lifetime.